Electrochemical Society

Vol. 99

UNIV. OF MICHIGAN
MAR 11 1952
EAST ENGINEERING
LIBRARY

1902—FIFTIETH ANNIVERSARY—1952

Electrothermics Issue

Uniformity

GLC Anodes for the electrolytic industry are uniform—they stand the test of comparison.

Baking Furnaces
Morganton,
N. C. Plant

Plants:
Niagara Falls, N. Y.
Morganton, N. C.

Great Lakes Carbon Corporation

GLC

ELECTRODE DIVISION · NIAGARA FALLS, N. Y.

Sales Offices:
Niagara Falls, N. Y.
New York, N. Y.
Chicago, Ill.
Pittsburgh, Pa.

Representatives:
Birmingham, Ala.
Wilmington, Cal.

PRODUCTS OF GREAT LAKES CARBON CORPORATION

Electrode Division
Graphite anodes. Graphite and amorphous carbon electrodes. Carbon and graphite specialties.

Oil and Gas Division
Crude petroleum and natural gas.

Carbon Division
Petroleum coke. Calcined petroleum coke. Industrial carbons.

Dicalite Division
Diatomaceous silica for filter-aids, fillers and insulating uses.

Perlite Division
Perlite lightweight aggregates and products for the building, oil, foundry and other industries. Perlite ore.

Merchant Coke Plant
Premium foundry and industrial coke. Coke co-products.

Journal of the

Electrochemical Society

MARCH, 1952 VOLUME 99 • NUMBER 3

CONTENTS

Anniversary Features

The Society and Electrothermics—Editorial. *C. H. Chappell* 49C
Electric Furnace Silicon Carbide Production. *G. M. Butler* 51C
Carbon and Graphite Electrodes. *C. G. Ollinger* 54C
Arc Furnace Practice in the Manufacture of Aluminous Abrasives and Refractories. *John A. Upper* 56C
New Refractories—Carbides, Borides, Nitrides, Silicides. *G. R. Finlay* .. 58C
Electric Furnace Phosphorus Development. *Walter Wallace* 60C
Electric Furnace Ferro-Alloys and Calcium Carbide. *Joseph H. Brennan* 61C
Electric Furnaces in the Iron and Steel Industry. *H. S. Newhall* 63C
Electric Furnaces for Melting of Nonferrous Metals. *G. H. Clamer* 65C

Technical Papers

Production of Titanium Ingots by Melting Sponge Metal in Small Inert-Atmosphere Arc Furnaces. *W. E. Kuhn* 89
Development of Graphite Electrodes and Study of Heat Losses with Different Electrodes in the Single Electrode Inert-Atmosphere Arc Furnace. *W. E. Kuhn* 97
The Relationship of Alpha and Beta Silicon Carbide. *Henry N. Baumann, Jr.* 109
The Synthesis, Fabrication, and Properties of Beryllium Carbide. *John H. Coobs and Walter J. Koshuba* 115
A Spectrophotometric Study of the Oxidation of Tantalum. *J. T. Waber, G. E. Sturdy, E. M. Wise, and C. R. Tipton, Jr.* 121

Current Affairs

Anniversary Meeting Expected to Set Record 69C
Division and Section News 70C
Personals 72C
New Members 73C
Book Review 74C
Literature from Industry 74C

EDITORIAL STAFF

R. M. BURNS, *Chairman*

NORMAN HACKERMAN, *Technical Editor* ELEANOR REID, *Managing Editor* F. L. LAQUE *Business Manager*
CECIL V. KING, *Associate Editor* MARY F. MURRAY, *Assistant Editor* U. B. THOMAS, *News Editor*

DIVISIONAL EDITORS: M. A. STREICHER, *Corrosion*; ABNER BRENNER, *Electrodeposition*; N. C. CAHOON, *Battery*; H. C. FROELICH, *Electronics*; W. C. GARDINER, *Industrial Electrolytic*; S. J. SINDEBAND, *Electrothermic*; R. R. RALSTON, *Electric Insulation*; L. B. ROGERS, *Theoretical*; SHERLOCK SWANN, JR., *Electro-Organic*

REGIONAL EDITORS: JOSEPH A. SCHULEIN, *Pacific Northwest*; J. C. SCHUMACHER, *Los Angeles*; O. W. STOREY, *Chicago*; G. W. HEISE, *Cleveland*; PAUL S. BRALLIER, *Niagara Falls*; OLIVER OSBORN, *Houston*; EARL A. GULBRANSEN, *Pittsburgh*; J. W. CUTHBERTSON, *Great Britain*; T. L. RAMA CHAR, *India*

ADVERTISING: Richard Rimbach Associates—James Condon. 133 Marlborough St., *Boston;* Richard Rimbach, Jr., 551 Fifth Ave., *New York;* William J. Gallagher. 3701 N. Broad St., *Philadelphia;* C. F. Goldcamp, 921 Ridge Ave., *Pittsburgh;* Harold Haskett, 360 N. Mich. Ave., *Chicago;* James R. Wright, 411 N. Tenth St., *St. Louis;* M. D. Pugh. 2721 N. Marengo Ave., *Altadena (Los Angeles).*

Published monthly by The Electrochemical Society, Inc., Mt. Royal and Guilford Aves., Baltimore 2, Md., combining the JOURNAL and TRANSACTIONS OF THE ELECTROCHEMICAL SOCIETY. Editorial Office: 235 W. 102nd St., New York 25, N. Y. Business Office: Mt. Royal and Guilford Aves., Baltimore 2, Md., or 235 W. 102nd St., New York 25, N. Y. Statements and opinions given in articles and papers in the JOURNAL OF THE ELECTROCHEMICAL SOCIETY are those of the contributors, and The Electrochemical Society assumes no responsibility for them. Subscription: $8.50 to members, $12.00 to nonmembers. Single copies $1.00 to members, $1.25 to nonmembers. Copyright 1952 by The Electrochemical Society Inc. Entered as second-class matter November 15, 1947, at the Post Office at Baltimore, Md., under the act of August 24, 1912.

What kind of men?

What kind of men are the 2500 scientists and engineers of Bell Telephone Laboratories?

They are men of many types, yet they work well together, for all have good minds as a foundation, years of study in the fundamentals of their science and in the methods of research and design. Vital, too, is their teamwork -- for without the co-operation of many individuals the products of research and development could never be perfected.

Above all else these men have "the spirit to adventure, the wit to question, and the wisdom to accept and use."

Such men can develop the world's finest telephone systems -- and have done so.

Perhaps there is a place among them for you. Write the Employment Director, Bell Telephone Laboratories, New York 14.

BELL TELEPHONE LABORATORIES

• EXPLORING AND INVE[illegible]TING, DEVISING AND PERFECTING FOR CONTINUED IMPROVEMENTS AND ECONOMIES IN TELEPHONE SERVICE

Production of Titanium Ingots by Melting Sponge Metal in Small Inert-Atmosphere Arc Furnaces[1]

W. E. Kuhn

Titanium Alloy Manufacturing Division, National Lead Company, Niagara Falls, New York

ABSTRACT

Two laboratory arc furnaces are described in detail. These furnaces were used to make ingots having diameters of 2½, 3, and 5 inches, and weighing up to 6 pounds.

Satisfactory melting of titanium sponge in the inert atmosphere arc furnace using nonconsumable electrodes is limited to sponge low in magnesium chloride, because the presence of entrained chloride causes spattering of the molten titanium onto the electrode tip, and contamination of the melt by the electrode material.

Graphite sleeves lining the inside of the water-cooled crucibles of small inert-atmosphere arc furnaces improve the melting efficiency but result in a prohibitively high carbon pickup. The carbon pickup tends to decrease as the diameter of the graphite-lined crucible increases.

Alternating current arcs in the inert-atmosphere arc furnace may be stabilized by superimposing a high frequency high voltage current on a low voltage alternating current supply. The indications are that neither tungsten nor graphite may be used for electrode tips with alternating current arcs because of the high losses of electrode material.

Introduction

Simply constructed laboratory arc furnaces designed and in use at these Laboratories have proved very successful for making small experimental melts of titanium and its alloys. It is hoped that some of the features embodied in the design of these furnaces may be of interest to others working with similar equipment. This paper provides: (*a*) details of simple, practical designs for laboratory arc furnaces; (*b*) a description of a practical method of melting sponge titanium without contamination; and (*c*) changes in furnace design for faster melting, and a discussion of the possibility of using alternating current instead of direct current for the arc.

Résumé of Development of the Inert Atmosphere Arc Furnace

For the sake of completeness of this paper, a résumé of the development of the inert-atmosphere arc furnace is included for the convenience of those not in a position to consult the references.

Perhaps the first arc furnace in this country, if not in the world, was invented by Robert Hare about 1839 (1). It is interesting to note that this furnace incorporated in its construction many of the features of the inert-atmosphere arc furnaces described in the literature and in this report. Vertically opposed electrodes were enclosed in a glass bell-jar which could be evacuated and into which various gases could be introduced. Materials to be reacted or melted were placed on a platform of charcoal supported by the lower electrode. The upper electrode consisted of a rod capable of vertical motion and which had an inverted cone of charcoal attached to its lower end. Power was supplied from a bank of large batteries. With this apparatus, Hare welded metallic electrodes together, melted instantly a platinum electrode a quarter of an inch in diameter, and performed many other interesting experiments.

The process of arc melting a refractory metal in the form of a consumable electrode on a water-cooled copper surface was developed by von Bolten in 1903 (2). Uranium metal in the form of a consumable electrode was melted by Moore about 1923 on a water-cooled Monel table with an arc in an atmosphere of argon at a pressure of 50 to 100 microns (3). Kroll modified the furnace of von Bolten by substituting a tungsten electrode for the consumable type electrode (4). Commercial application of this method was finally made about 1937 when the M. W. Kellogg Company developed the "electric ingot" process for the production of special high quality alloy steels (5). This furnace used a consumable type electrode and a water-cooled mold. A similar type of furnace operating under a vacuum and using consumable electrodes and a water-cooled copper mold was developed by Parke and Ham at the Climax Molybdenum Company (6). Herres and Davis at Battelle Memorial Institute further developed the Kroll-von Bolten method by using a water-cooled tungsten tipped electrode for melting titanium and other reactive and nonreactive metals in a water-

[1] Manuscript received June 20, 1951. This paper prepared for delivery before the Washington Meeting, April 8 to 12, 1951.

cooled copper crucible under an inert atmosphere of argon or helium (7).

The general principles of operation are incorporated in the following descriptions of the furnace, and also may be found in References 4–10.

Two arc furnaces were designed and built. One of these furnaces, built primarily for the purpose of making small melts of titanium and zirconium and

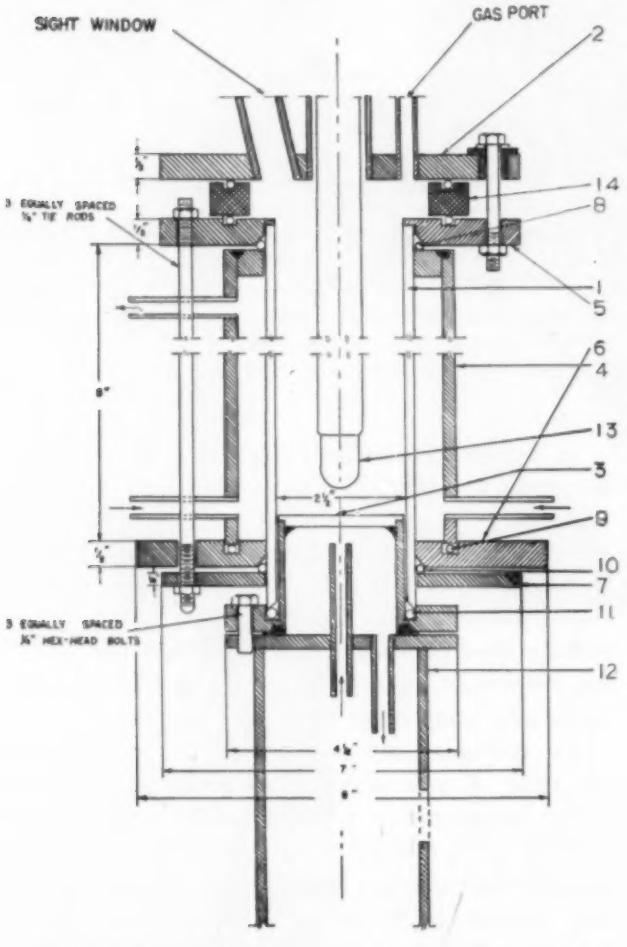

FIG. 1. 2½-Inch inert-atmosphere arc furnace. 1—Water-jacketed copper crucible, 2—cover, 3—water-cooled bottom plate, 4—4-inch diameter steel pipe, 5—upper flange, 6—lower flange or base plate, 7—pressure ring, 8—Linear* O-ring 1820-39, 9—Linear O-ring 1820-48, 10—Linear O-ring 1820-39, 11—Linear O-ring 1820-36, 12—3½-inch steel pipe support, 13—tungsten tip, 14—fiber insulation.

* Available from Linear, Incorporated, State Road and Levick Street, Philadelphia 35, Pennsylvania.

base alloys of these metals weighing up to about 200 grams, employs a 2½-inch diameter crucible. The other furnace is used for making larger ingots weighing up to several pounds in either a 3- or 5-inch diameter crucible. Since the larger furnace duplicates most of the features possessed by the 2½-inch diameter furnace, the details of only the latter furnace are described here.

Design Considerations of a 2½-Inch Diameter Arc Furnace

Special consideration was given to the efficient and rapid production of small melts of titanium and titanium base alloys. It was decided that such a furnace could be constructed by incorporating the following features:

1. Simple construction to facilitate (*a*) rapid cleaning of interior surfaces, (*b*) rapid removal of melted charge, and (*c*) rapid replacement of damaged furnace parts.
2. Standard sized O-ring type vacuum seals.
3. Sight-window for observing the arc and the melting metal.
4. Replaceable crucible walls and bottom.
5. Simply designed electrode and cable holder such that dismantling of the furnace and replacement of the electrodes is facilitated.
6. Automatic rotary oscillation of the electrode with its tip offset so that the arc moves in a 360° circle approximately one-half inch from the sides of the crucible.
7. Arc length manually controlled by hand crank or lever.
8. Both vertical and horizontal movement of the furnace crucible with respect to the electrode to facilitate cleaning, removal of melted metal, and furnace repairs.
9. Electrode tips which can be readily replaced without removing the copper electrode from its holder. The use of replaceable graphite tips is described in Reference 11. It is reasonable to assume that replaceable tungsten tips could also be used with a water-cooled electrode holder of special design.

Description of the Furnace

The furnace (Fig. 1) consists of a water-jacketed hollow cylinder (1), a cover (2), and a water-cooled bottom plate (3).

The furnace cover (2) incorporates the sight-window, the opening and vacuum seal for the electrode, and the connection for vacuum and gas supply systems. The cover is electrically insulated from the water-jacketed crucible by means of a spauldite[2] ring and insulated bolt holes. Two "O" ring gaskets on either side of the spauldite ring provide a vacuum seal.

The water-jacketed cylinder (1) consists of a length of standard 2½-inch copper pipe having a wall thickness of about ¼ inch. A length of 4-inch steel pipe (4), concentric with the copper pipe (1) and having an inside flange welded at the top, forms the outer walls of the water jacket. Tie-rods are used to pull

[2] An insulating material consisting of canvas layers impregnated and bonded with varnish.

the upper and lower flanges (5) and (6), respectively, and the pressure ring (7) together. The "O" ring seals at (8), (9), and (10) make the equipment both water and vacuum tight. When the tie-rods are fully tightened, the copper cylinder is very tightly held in position by the "O" ring gaskets.

The bottom plate (3) consists of a copper plate brazed to a short length of pipe. A steel plate bolted to a flange welded to the steel pipe carries the inlet and outlet ports for the cooling water. Replacement of a burned-out bottom plate (3) is made by simply removing the damaged one and replacing it with a new one. However, by using a copper plate one or more inches thick, repairs to a badly pitted plate are facilitated and the life of the plate prolonged by simply turning off the damaged layers of copper. The bottom plate assembly (3) is supported on top of a length of 3½-inch steel pipe (12).

All the steel parts of the furnace—parts (2), (3), (4), (5), (6), and (7) are nickel plated to prevent corrosion and to facilitate cleaning.

The furnace is mounted on a drill press. The vertical and rotary motions of the spindle were used for both vertical control and rotation of the electrode. An electric motor and gear reduction unit is used to give an oscillatory rotation to the electrode of one complete turn of 360° per minute.

Details of the electrode holder are shown in Fig. 2. The electrode holder and electrode are attached to the spindle movement of the drill press mounting by means of a tapered member (1) which fits into a tapered chuck and is locked in place by means of a set screw. The copper electrode is screwed into a flanged pipe coupling (6) bolted to the electrode holder. This coupling acts as the upper seal for the flexible rubber tube connecting with the furnace cover. The electrode is electrically insulated from the drill press mounting by a spauldite plate (3) and insulated bolt holes in the upper flange. The power cable to the electrode is connected to the holder by means of a solderless type cable clamp bolted to the lower flange plate (4). That part of the furnace comprising the cover and water-jacketed copper cylinder is mounted on the work table of the drill press and the water-cooled bottom plate assembly (3) is fixed to the frame. Thus, to effect a vacuum seal between the upper and lower parts of the furnace, the upper part is lowered down onto the bottom plate so that the bevelled bottom edge of the 2½-inch copper tube is pressed against the "O" ring at (11).

A diagram of the furnace, vacuum system, water-cooling system, inert gas supply, and electrical connections is shown in Fig. 3.

Cleaning of the furnace is accomplished by running a rotating wire brush through the copper tube, wiping out the crucible first with a water-soaked rag and then an acetone soaked rag. The furnace is then prepared for melting, and evacuated. Live steam injected into the cooling water supplied to the furnace

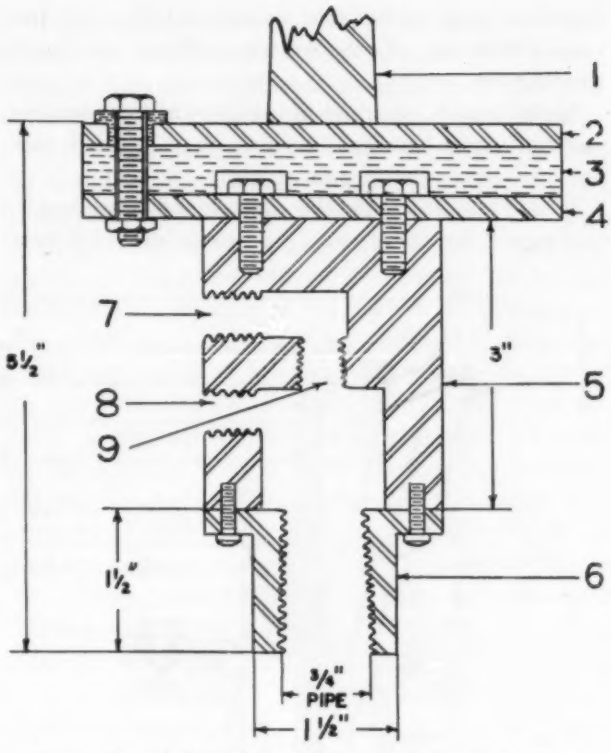

FIG. 2. Electrode holder for water-cooled tungsten-tipped electrodes. 1—Tapered connection, 2—upper flange, 3—insulation, 4—lower flange, 5—brass, 6—flanged ¾-inch pipe coupling, 7—inlet for cooling water, ¼ ips, 8—outlet for cooling water, ¼ ips, 9—connection for pipe leading cooling water to tungsten tip, ¼ ips.

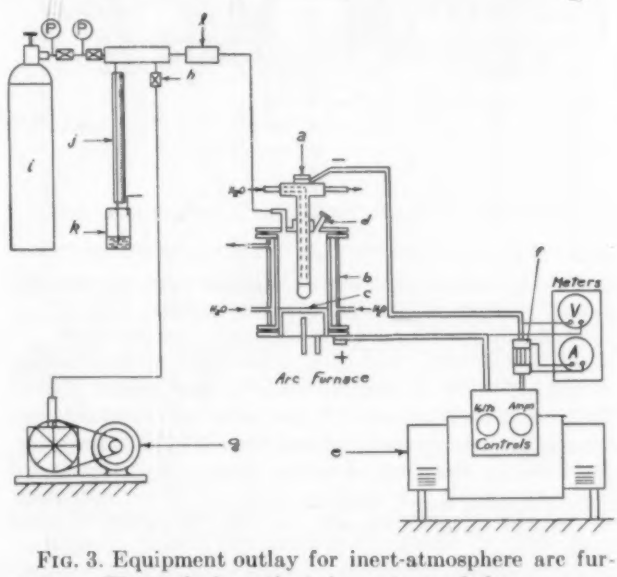

FIG. 3. Equipment outlay for inert-atmosphere arc furnace. a—Electrode (negative), b—water-cooled copper crucible, c—water-cooled bottom plate, d—sight window, e—600-amp welding generator, f—1000 amp-50 mv shunt, g—mega-vac pump, h—vacuum valve, i—inert gas supply, j—Hg manometer, k—Hg bubbler, l—gas filter.

insures a completely dried furnace interior and prevents sweating of the outer surfaces in humid weather.

Metal may be charged in the form of loose sponge, powder, small turnings or shot, or as pressed compacts of either powder or sponge.

It is possible, with the equipment described in this report, for one man to produce from 7 to 8 melts

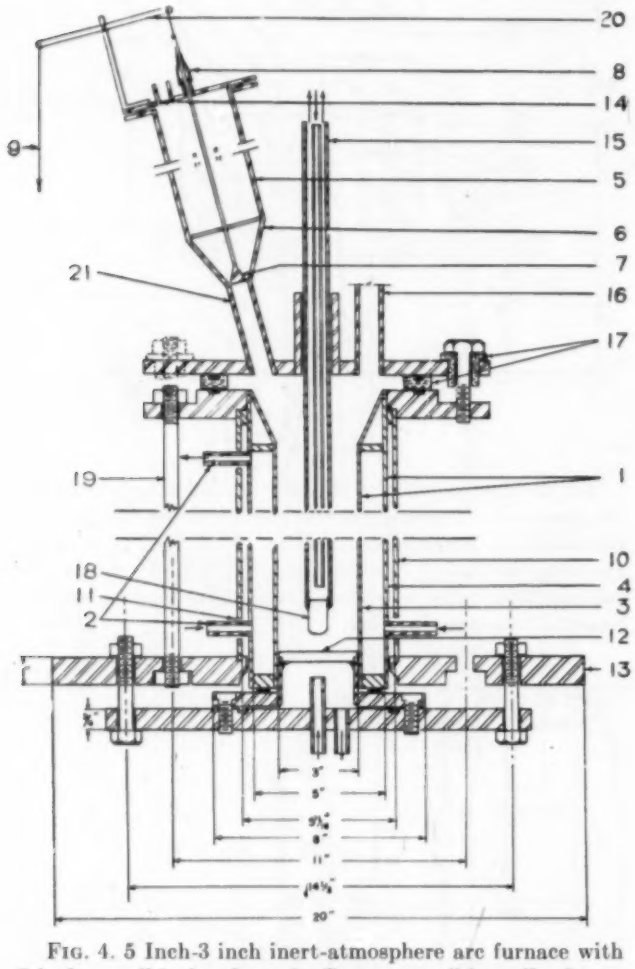

FIG. 4. 5 Inch-3 inch inert-atmosphere arc furnace with 3-inch crucible in place. 1—Copper crucible walls, 2—removable nipples for inlet and outlets for cooling water, 3—3-inch copper tube, 4—5-inch copper tube, 5—feed hopper, 6—cone, 7—bell, 8—flexible seal, 9—feed hopper control line, 10—6-inch diameter brass tube, 11—threaded pipe fitting, 12—water-cooled bottom assembly, 13—base plate, 14—inlet for charging titanium sponge, 15—water-cooled copper electrode, 16—sight window, 17—fiber insulation, 18—brazed tungsten tip, 19—tie rods, 20—lever, 21—feed tube.

in an 8-hour day, assuming no delays. It may be possible to increase the number of tests a day to about double by incorporating the following two additional features in the arc furnace design: (*a*) a multiple sample feed device capable of handling a large number of prepared samples, and (*b*) an enclosure of the lower part of the furnace so that test buttons may be unloaded from the bottom plate in an inert atmosphere. Contamination of the furnace by moisture and air would be avoided, thereby eliminating the need for frequent cleaning of the furnace.

Design of Arc Furnace Employing Either 5-Inch or 3-Inch Diameter Crucibles

The design of this furnace as it is used with a 3-inch diameter crucible is shown in Fig. 4. The crucible consists of a brazed double-walled, all-copper vessel (1) equipped with removable nipples (2) and a water-cooled bottom (12). Except for minor modifications, the design of this furnace when used with a 5-inch diameter crucible differs little from the description already given for the 2½-inch diameter furnace.

This furnace is mounted on a drill press in much the same manner as the 2½-inch diameter furnace. The horizontal swing table of the drill press is used to move the entire furnace from beneath the spindle carrying the electrode for cleaning or repairs.

As with the 2½-inch furnace automatic oscillatory rotation of the electrode (15) is provided for and the arc length is controlled by vertical movement of the spindle. Operation of the larger furnace by one person is very much facilitated by this feature.

Control over the amount of sponge charged to the furnace is accomplished by the bell and cone feed hopper (5), Fig. 4. Upward movement of the bell (7) within the cone (6) allows the crushed and sized sponge to fall freely into the furnace in readily controlled amounts. The flexible seal (8) is under slight tension when the hopper opening is closed, thus insuring that the cone (7) returns to the closed position when the control line (9) is released.

When it is desired to use the furnace for melting 5-inch diameter ingots, the 3-inch diameter crucible is removed and a standard length of 5-inch diameter copper tubing is installed in the same manner that the 2½-inch copper tube is with the 2½-inch furnace. The outer 6-inch diameter tube (10) then becomes the outer wall of the water-jacket. The openings through which the nipples for the three-inch crucible are inserted (11) are threaded pipe fittings which may also be used for connecting the inlet and outlet nipples for the 5-inch diameter crucible.

To remove the ingot, the entire furnace is swung to one side and the platen of a small hydraulic jack brought up against the bottom of the water-cooled bottom plate assembly (12). Then the bolts holding the bottom plate (12) to the base plate (13) are removed and the whole bottom plate assembly and ingot are gently lowered by the hydraulic jack.

Manometers are used to measure water flow rates to the water-cooled parts of the furnace.

The main advantage of having a furnace such as this is to have available arc melting equipment for

making both large and small experimental melts with the minimum of equipment, space, and cost.

Arc Melting Titanium Sponge

Preliminary to melting, the interior surfaces of the furnace are first thoroughly cleaned. Then, with the furnace cover and bottom firmly bolted in place, the feed hopper is filled with an amount of sponge equal to that of the desired weight for the ingot. A small amount is allowed to drop through onto the water-cooled bottom as a starting charge. The charging hole in the lid of the hopper (14), Fig. 4, is then sealed and the furnace swung into position axially beneath the spindle of the drill press. The electrode, already in position as shown in Fig. 4, is moved upward into its tapered connection. The furnace is now ready for evacuation and flushing.

Just before melting, the furnace is evacuated to within about a millimeter of mercury pressure and then flushed with argon gas. Evacuation and flushing are repeated one or two more times. Before the last flush, the leak rate is measured. If no change in the vacuum greater than about one millimeter of mercury occurs over a period of four to five minutes, the furnace is regarded sufficiently vacuum-tight for operation. The furnace is then filled with argon and the pressure maintained slightly above atmospheric by the small pressure head in the mercury bubbler (k), (Fig. 3).

Special purity argon of the grade used for inert gas shielded arc welding is used.

Melting is started by igniting the arc on the loose sponge of the starting charge. When this is fully melted, additional sponge is charged at a rate compatible with complete and rapid melting. In this way, the ingot is progressively built up by incremental charging into the arc during melting until the hopper is empty.

Using tungsten-tipped electrodes and arc currents between 300 and 500 amperes direct current and voltages between 24 and 30 volts, a number of ingots weighing five to six pounds were produced from high chloride sponge in the 3-inch diameter crucible. Sponge titanium crushed and sized to minus $\frac{1}{2}$ inch and plus $\frac{1}{4}$ inch was used for feed.

Some of the results obtainable using those low currents are given in Table I.

Recoveries on six of the above ingots after grinding, forging, and rolling into strip ranged from 51 to 90 per cent with an average recovery of 75 per cent. These recoveries depended largely upon the surface condition of the ingot, which, in turn, depended on the amount of spatter during melting, and the size of the increments charged into the furnace.

In all the melts of Table I, the electrode tip was offset from its axis in such a way that the molten pool covered the entire surface of the melt during a single 360° oscillation. When currents of 900 amperes or more are employed, straight electrodes may be used with a 3-inch crucible, and such high currents are practical without crucible failures by arcing and burning through the crucible walls if the sponge melted is free from chlorides.

A rapid flow of water about the copper crucible is required at the higher currents to prevent the formation of steam pockets at the surface of the copper. The steam prevents the rapid removal of heat and causes the copper to melt through in the vicinity of the arc. On one occasion, a failure of this type occurred in the crucible wall at a point well below the top level of the molten metal causing the steam to channel its way to the surface of the ingot. The presence of very small amounts of water results in high arc voltages and generally causes the arc to go out. These characteristics provide an automatic warning and safety device in the event of internal leaks in the water-cooling system of the furnace.

TABLE I. *Results of experimental production of titanium ingots by melting sponge in the 3-inch arc furnace*
Arc current 300–500 amperes (direct current)

Lot designation of sponge	No. of ingots	Melting rate lb/hr	% W in the ingots	Remarks
A	2	3 to 4	Undetected	Exceedingly little spatter
B	2	1.5 to 1.8	0.001 to 0.05	Metal spattered
C	4	0.8 to 1.4	0.001 to 0.05	Metal spattered
D	4	0.9 to 2.0	0.001 to 0.05	Metal spattered
E	2	0.9 to 1.5	0.001 to 0.02	Metal spattered

Improving Titanium Sponge for Melting

It was observed early that melts containing chlorides spattered titanium over the electrode and interior of the furnace. This generally resulted in high tungsten contamination of the melts and frequent arcing through the crucible walls. Therefore, a number of experiments were made to determine more precisely the effect of the $MgCl_2$ in the sponge on arc melting practice.

Leaching experiments with fine and coarse sponge indicated that the chloride content of the finer sponge was greater than that of the coarser. Coarse sponge was found to melt with less spatter than fine sponge. This suggested that sudden release of the water of hydration in entrapped $MgCl_2$ under the intense heat of the arc caused the severe spattering. The contamination of the melted metal with tungsten from the electrode may be explained by the formation on the electrode of a low melting point alloy of titanium with the tungsten which drops off

into the melt. The amount of moisture that can be derived from the air is indicated by the following experiment. Two samples of titanium sponge, dried at 110°C and containing approximately 0.07 and 0.35 per cent chlorides as $MgCl_2$, were exposed to air (humidity 68% at 66°)F. After exposure of one hour, weight increases of 0.18 and 0.68 per cent, respectively, were observed. After five hours these weight increases were 0.19 and 0.86 per cent, respectively. These data merely serve to emphasize the need for the immediate storage of sponge titanium in a dry atmosphere after it is removed from the reaction vessel. Similar experience with $MgCl_2$ was reported by Maddex and Eastwood (13).

TABLE II. *Effect of leaching of sponge on hardness after fusion*

Experiment	Brinell hardness of fused button	Preliminary treatment of sponge
1	363	Not leached
2	269	Leached for 7 hours in water and dried at 120°C
3	217	Leached for 7 hours in water and dried at 120°C
4	269	Leached for 7 hours in water and dried at 120°C

TABLE III. *Results obtained in melting titanium sponge in an inert-atmosphere arc furnace lined with graphite*

Melt No.	Inside diameter inches		Current used amp	Melting rate lb/hr	Ingot produced			Type of graphite used for liner
	Copper crucible	Graphite liner			Weight lb	Carbon content %	Brinell hardness	
1	2⅞	2½	240/600	1.7	2¼	1.02	263	Porous
2	2⅞	2½	240/600	1.9	2¼	1.19	212	Porous
3	2⅞	2½	240/600	2.2	2¼	1.40	254	Dense
4	5	4¼	500/600	3.5	4	0.56	281	Dense

TABLE IV. *Carbon distribution in cross sections of ingots melted in graphite-lined crucibles in 3-inch furnace*

Melt No.	Distance from periphery of ingot				Average
	Surface	¼ in.	½ in.	Center	
1	1.03	0.94	1.00	1.11	1.02
2	1.19	1.16	1.20	1.19	1.19
3	1.76	1.52	1.38	0.95	1.40

The influence of leaching of sponge to remove $MgCl_2$, and drying at 120°C, on the hardness after melting is indicated in Table II.

Although these results indicate a substantial lowering of the hardness of the fused titanium, there was little reduction in the amount of spattering after leaching and drying.

Methanol has also been employed for leaching, and has been found to have a slight advantage over water insofar as the last traces of solvent are more easily removed from the sponge (8, 9).

In summary, the best possible melting quality is attained in titanium sponge only through the complete removal of chlorides in the reduction process. If chlorides are present, they must not be given an opportunity to hydrolyze because ultimate removal of either the hydrous chloride or its water of hydration is both difficult and costly, and any oxide present in the chloride becomes available to the titanium on melting, increasing its hardness and brittleness.

Today most of the sponge produced is low in chlorides so that arc melting is relatively free from the difficulties ascribed to chloride contamination, and leaching is seldom required.

The Use of Graphite Sleeves

A number of melts were made to determine the practicability of using graphite liners to reduce heat losses and thereby increase the melting rate. The results of these experiments are reported in Tables III and IV.

Some increase in melting rate is to be noted in comparing Table IV with most of the results in Table I, but this advantage is offset by the large amount of carbon introduced into the metal. In the 3-inch furnace, it was observed that the arc displayed a tendency to direct itself close to one side of the crucible. The graphite on this side, being considerably hotter than at any other part of the sleeve, became wetted and was rapidly dissolved by the titanium. In the 5-inch furnace, this difficulty was not experienced, and consequently, the carbon pickup was reduced by over 50 per cent.

The graphite sleeves could be readily chipped or sand-blasted off, leaving a smooth finish at the surface of the ingot.

Kroll and Gilbert (14) successfully arc melted zirconium in an all-graphite crucible with little carbon pickup from the crucible. This, as observed by Anderson, *et al.* (15), and Kuhn (11) is due to the considerably greater passivity of molten zirconium toward graphite, as compared with that of titanium. It is probable, therefore, that considerably less contamination would have resulted if zirconium, rather than titanium, had been melted in the graphite-lined furnace.

The carbon distribution in Ingots 1 and 2 was reasonably uniform, but in Ingot 3 the carbon increased greatly from the center to the periphery. The reason for this difference in the carbon distribution is not known, but is probably related to melting practice.

Stabilized a-c Arcs for Melting Metals in the Inert Atmosphere Arc Furnace

A few experiments were conducted in the 5-inch diameter furnace to determine the feasibility of melting titanium using alternating current supplied by a 30-kva furnace transformer.

An initial series of melting experiments using straight a-c power at voltages from 40 to 120 volts and currents up to 1000 amperes failed to produce a stable arc. Experiments by Davis, Herres, and Greenidge showed that an alternating current arc could be stabilized by superimposing a high-frequency current on the current obtained from a transformer (12).

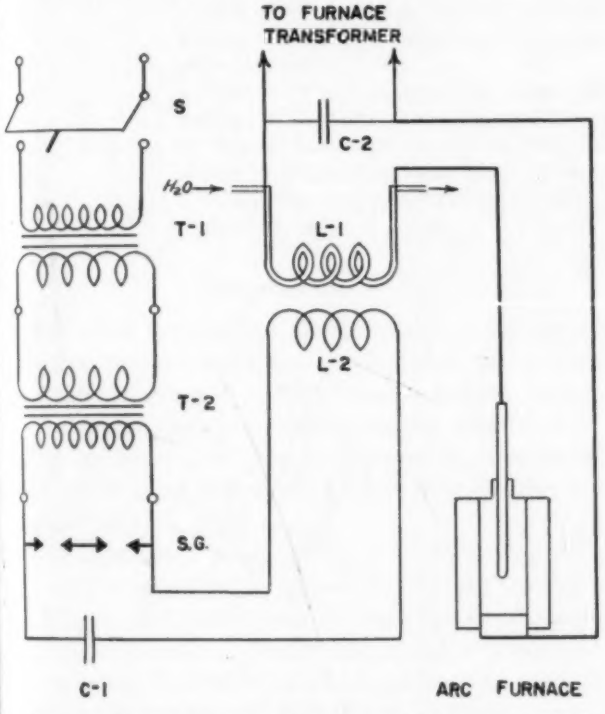

Fig. 5. Circuit diagram for arc stabilizer. S—Switch, T-1—step-down transformer, primary 110 volts, secondary, 25,000 volts, S.G.—double spark gap with tungsten tips, C-1—0.003 μfd, C-2—5 μfd, L-1—10 turns ¾-inch diameter copper tubing, L-2—8 turns, No. 8 copper wire.

The voltage necessary for re-ignition of an arc across a gap depends largely on thermal conditions at the electrodes and within the gap; hence, a mean effective voltage high enough to re-ignite the arc at minimal thermal conditions must be employed. Since the voltages required for a stabilized arc could not be obtained with the furnace transformer being used in these experiments, an arc stabilizer of the design shown in Fig. 5 was constructed. This arc stabilizer consists of a high voltage a-c supply, a double spark-gap oscillator, a coupling coil for introducing the high-frequency high voltage power into the arc furnace, and a by-pass condenser for keeping the high frequency current out of the furnace transformer to avoid a possible breakdown.

Stabilized arcs were successfully obtained using the arc stabilizer described above. The only serious objection to this type of stabilizer is its erratic behavior when not properly adjusted. A radio frequency high voltage stabilizer which operates more quietly and smoothly would be far more satisfactory.

Determinations by various investigators indicate maximal temperatures from 4700° to 7000°K and minimal temperatures of 3550° to 5000°K for the a-c arc (16). These temperatures are substantially higher than those encountered at the cathode of a d-c arc estimated to be between 3000° and 3500°K. In these experiments, the bare graphite-tipped electrodes used exhibited severe erosion by the a-c arc and undoubtedly introduced a considerable amount of carbon into the melt. It has also been shown that considerable tungsten is consumed when either iron or titanium are melted using a water-cooled tungsten tipped electrode and alternating current for the arc (12). Because of the higher electrode temperatures, it will be difficult to find a material sufficiently refractory to be used as a nonconsumable electrode tip material with a-c arcs. However, there is good reason to believe that a-c power could be successfully applied to arc melting with consumable electrodes made of the metal to be melted.

Acknowledgment

The author wishes to express his appreciation to the management of the Titanium Alloy Manufacturing Division of the National Lead Company for permission to publish the results of this investigation. The counsels and criticisms of Dr. S. F. Urban, Director of Research, Mr. G. F. Comstock, Assistant Director, and Mr. R. S. Stewart, Assistant Chief, Physical Metallurgy Division, have been invaluable to the author. Particular thanks are due to those who assisted in the experimental work, namely, Mr. E. Johnson who gave most valuable help to the author throughout the investigation, Mr. G. Dorso of the Electrical Maintenance Department, and Messrs. A. Hudson, J. Reynolds, and E. Wick of the Research Laboratory staff.

Any discussion of this paper will appear in a Discussion Section, to be published in the December 1952 issue of the Journal.

References

1. C. A. Doremus, *Trans. Electrochem. Soc.*, **13**, 347 (1908).
2. C. W. Balke, *Chemistry & Industry*, **1948**, 83.
3. R. W. Moore, *Trans. Electrochem. Soc.*, **43**, 317 (1923).
4. W. J. Kroll, *Trans. Electrochem. Soc.*, **78**, 35, (1940).
5. W. R. Clauser, *Materials & Methods*, **27**, No. 1, 57 (1948).

6. R. M. Parke and J. L. Ham, *Metals Technol., Tech. Publ. No. 2052*, **13**, (6) (Sept. 1946).
7. S. A. Herres and J. A. Davis, *Steel*, **124**, No. 18, 82 (1949).
8. O. W. Simmons, C. T. Greenidge, and L. W. Eastwood, "Titanium—Report of Symposium Sponsored by O. N. R.," p. 77, (1948); *Metal Progress*, **55**, 197 (1949).
9. C. M. Craighead, O. W. Simmons, and L. W. Eastwood, *Trans. Am. Inst. Mining Met. Engrs. (also J. Metals)*, **188**, 485 (1950).
10. L. W. Eastwood and C. M. Craighead, Air Force Technical Report 6218, Vol. **11** (1950).
11. W. E. Kuhn, *J. Electrochem. Soc.*, **99**, 97 (1952).
12. J. A. Davis, S. A. Herres, and C. T. Greenidge "Arc Melting of Titanium and Titanium-Base Alloys at Battelle Memorial Institute, Rand Report R-131," Battelle Memorial Institute, Columbus, Ohio (March 15, 1949).
13. P. J. Maddex and L. W. Eastwood, *Trans. Am. Inst. Mining Met. Engrs. (also J. Metals)*, **188**, 634 (1950).
14. W. J. Kroll and H. L. Gilbert, *J. (and Trans.) Electrochem. Soc.*, **96**, 158 (1949).
15. C. T. Anderson, E. T. Hayes, A. H. Roberson, and W. J. Kroll, "A Preliminary Survey of Zirconium Alloys," *U. S. Bur. Mines Repts. Invest. 4658* (1950).
16. W. Spraragen and Bela A. Lengyel, *J. Am. Welding Soc. Research Supplement*, **8**, No. 1 (Jan. 1943).

Development of Graphite Electrodes and Study of Heat Losses with Different Electrodes in the Single Electrode Inert-Atmosphere Arc Furnace[1]

W. E. Kuhn

Titanium Alloy Manufacturing Division, National Lead Company, Niagara Falls, New York

ABSTRACT

A titanium-TiC coated graphite-tipped electrode was developed for melting titanium without excessive carbon pickup. The principles evolved from the melting of titanium and zirconium may be extended to the development of graphite tips coated with other carbide-forming elements.

The effect of varying arc length, arc current, and arc voltage on the steady-state heat losses in the cooling water supplied to the electrode, crucible walls, and crucible bottom were studied.

Electrode and bottom heat losses increased linearly with increasing current and amounted to about 10 and 4 per cent, respectively.

Heat extracted by the crucible walls amounted to about 80 per cent of the total power input. Short arc lengths and high arc currents tended to improve the melting efficiency.

Tungsten-tipped electrodes exhibited more efficient arc melting characteristics than graphite tips.

Introduction

The chief function of the electrode in an inert-atmosphere arc furnace is to conduct electrical energy into the furnace and there release it as heat energy to the melt in the most efficient manner possible. Not all of the heat is utilized in the process of melting, for some is used wastefully in the electrode, the arc plasma, and the melt.

The number of ways by which heat developed at the cathode spot is dissipated by the electrode are as follows: (*a*) conduction through the electrode to the holder or cooling water, (*b*) escape of electrons, (*c*) radiation to interior surfaces of the furnace, (*d*) gaseous conduction and convection, and (*e*) evaporation of cathode material.

In addition to the above losses, heat generated in the electrode by virtue of its electrical resistance is dissipated in the electrode holder or cooling water.

Two types of electrodes are suggested by consideration of the above factors: (*a*) Electrodes which utilize some of the heat losses. Maximum use of the losses may be realized in a consumable electrode consisting of the material to be melted. (*b*) Electrodes which do not utilize the heat losses. Since these losses are not used, they must be minimized. Also, this type must be nonconsumable.

It is clear that a furnace employing consumable electrodes will be more efficient. However, where small laboratory arc furnaces are concerned, the increased efficiency resulting from the use of consumable electrodes cannot be justified because of their elaborate and costly construction. Furnaces employing nonconsumable electrodes are generally quite satisfactory for making laboratory-size melts.

[1] Manuscript received June 20, 1951. This paper prepared for delivery before the Washington Meeting, April 8 to 12, 1951.

Development of Graphite Electrodes

Nonconsumable Electrodes for d-c Arcs

The objective in the design of nonconsumable electrodes is to minimize heat losses in the electrode and loss of electrode tip material. Ohmic heat losses are minimized by making the electrode of a high conductivity material such as copper. Also, because the cathode spot is heated to a lower temperature than the anode, the electrode is made cathodic to minimize loss of electrode tip material and some of the other heat losses. Although high conductivity materials, in general, have low melting points, the electrode should be tipped with a material possessing as many as possible of the following properties:

1. High melting point and low vapor pressure at the temperature of the cathode spot, 3000°–4000°K.
2. Sufficiently high thermal conductivity for rapid heat transfer away from the cathode spot. This is necessary to prevent the melting of the cathode tip material.
3. Reasonably good electrical conductivity.
4. Good mechanical strength, particularly at high temperatures, to withstand mechanical abuse and fluctuating thermal stresses.
5. Ability to form a wide range of high melting point alloys when alloyed with the metal to be melted, but low solubility in the material to be melted at the melting point of the latter.

6. Ability to be joined by brazing, soldering, or welding, or to be machine fitted.

TABLE I. *Melting points of refractory elements and carbides*

Metals	Melting point °C	Carbides	Melting point °C
Tantalum	3000	HfC	3887
Tungsten	3410	TaC	3877
Graphite	3925 (begins to volatilize)	TiC	3137
		ZrC	3532

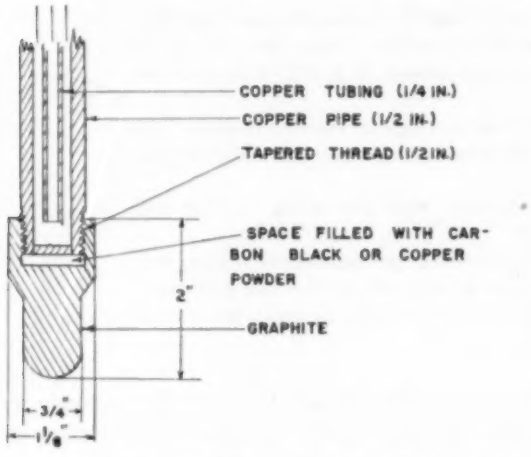

FIG. 1. Graphite tip and copper electrode for inert-atmosphere arc furnace.

TABLE II. *Melting experiments using graphite tipped electrodes*

Melt No.	Current amp	Melting time min	Titanium melted			Condition of tip
			Weight	Carbon content	Carbon pickup	
107	200/500	20	—	0.54	0.54	Tip not coated
111	280/500	16	—	0.66	0.63	Tip not coated
112	280/500	120	1 lb 5 oz	0.25	0.22	Partially coated tip
118	400	5	200 g	0.10	0.07	Coated tip
126	400	10	200 g	0.06	0.03	Coated tip*
127	400	15	200 g	0.05	0.02	Coated tip
128	400	20	200 g	0.04	0.01	Coated tip
129	500	10	250 g	0.06	0.03	Coated tip
130	600	10	250 g	0.03	0.00	Coated tip
131	500	10	250 g	0.04	0.01	Coated tip
132	400	10	250 g	0.08	0.05	Coated tip
119	400	21	316 g	0.03	0.00	Tungsten tip‡
108	400	201	3 lb	0.03	0.00	Tungsten tip
109	400	222	4¼ lb	0.03	0.00	Tungsten tip

* Same graphite tip used in Runs 123 to 132, inclusive. Total amount of material melted with this tip was 7¼ lb.

‡ Same lot of titanium sponge used throughout experiments 123 to 132, inclusive, and melts 108, 109, and 119.

Some of the metals and compounds possessing the more important of the above properties are listed in Table I. There are only two metals suitable for electrode tips, tungsten and tantalum, and, of these, tungsten has proved to be very satisfactory. Tantalum has not been tested but, other things being the same, could probably be used as a tip material with small arc currents. Bare graphite, despite its high melting point, introduces considerable carbon into the melt, but for certain applications the amount of carbon introduced might not be objectionable if it could be controlled within narrow limits below a maximum of, say, 0.4 per cent.

The use of such hard, brittle compounds as borides, nitrides, and carbides is precluded at this time by the difficulties of forming them into tips and joining them to the electrode. They are all brittle materials that do not withstand mechanical abuse particularly well.

General practice as reported in the literature is to use water-cooled copper electrodes with tungsten tips brazed or silver-soldered onto the ends. These have proved very satisfactory except under conditions where heavy spattering of titanium is encountered. Under these conditions the tungsten is slowly eroded away. When a spatter-free sponge is used, the amount of tungsten lost to the melt is small and innocuous. However, under conditions of severe spattering, tungsten has been found in the melt in the form of small chips or localized hard spots of high tungsten concentration.

In view of the difficulties with tungsten due to spattering, it was decided to investigate graphite as a tip material. An attractive feature of graphite is the facility with which burned-out electrode tips may be replaced when a threaded connection with the electrode is used. Also, because of the relatively high rate of solution of carbon in molten titanium, the formation of hard spots is less likely to be encountered with carbon than with tungsten.

Graphite Tips

Preliminary trials.—The graphite tip shown in Fig. 1 was used throughout the investigation of graphite-tipped electrodes. The electrode consists of a water-cooled copper pipe having a copper plug silver-soldered into one end. Both ends of the electrode are provided with standard pipe threads. The open end is screwed into the electrode holder and the graphite tip onto the plugged end. Carbon black or copper powder may be packed into the bottom of the threaded hole of the tip to provide better thermal and electrical contact between the tip and copper electrode. A dense form of graphite is preferred for the tips because of its higher mechanical strength.

The results of the first melting experiments are given in Table II. A large carbon pickup was obtained for the first three melts, the third of which gave a significantly lower carbon content. It was

noted that the low carbon melt was obtained with a tip that had become partially coated with titanium. From this, it was reasoned that a titanium coating might, by the formation of a high melting point carbide layer, serve as a diffusion and mechanical barrier to hinder the transport of carbon through the arc and into the melt. Fully coated graphite electrodes were thereupon prepared and tested with the results given in the lower part of the table. A pronounced drop in the carbon pickup was realized. Similarly, low carbon pickup was obtained in melting zirconium using zirconium-coated graphite tips, as shown in Table III.

It is reasonable to assume that hafnium- and tantalum-coated graphite tips would be even more effective than those coated with titanium or zirconium in preventing carbon pickup, because of the high melting points of hafnium and tantalum carbides, 3887° and 3877°C, respectively. No experience so far has indicated that such tips would show any superiority for melting titanium or zirconium, but it certainly would be worthwhile to try them for melting tantalum and hafnium.

Coating of graphite electrode tips.—In the preceding experimental work, the graphite tips were spatter-coated in the arc furnace by melting high chloride titanium sponge. As this method was time-consuming, a number of other methods were tried. A dip-coating technique, consisting of dipping the tip into molten titanium under argon in an induction furnace, fulfilled all practical requirements. After coating, the tips were conditioned in the arc furnace. The conditioning treatment consisted of making one or two melts with the tip for the purpose of melting off excess titanium and enriching the remainder with carbon. The carbon contents of the first two melts made with a series of newly-coated tips are given in Table IV. With one exception, the carbon pickup was reduced to a harmless amount in the first conditioning treatment. It is advisable to use the same current for conditioning as will be used for melting.

Structure of coated graphite tips.—A section of a coated graphite tip was examined with the microscope to determine the nature of the coating. The photomicrographs in Fig. 2 (*a*), (*b*), and (*c*) were taken at the points indicated on the sketch of a longitudinally sectioned tip. Three distinct layers were evident: a carbide layer adjacent to the graphite, and two layers (*b*) and (*c*) consisting of titanium carbide dendrites in a matrix of titanium containing carbon in solution. It is evident that, during melting with a graphite tip, the Ti-TiC alloy varies in composition over quite a wide range if a reasonably large amount of titanium spatters onto the tip.

The constitution diagram of titanium and carbon (1), although not firmly established, indicates that,

TABLE III. *Melting zirconium metal* in the arc furnace using a zirconium-coated graphite tip*

Melt No.	Current	Melting rate lb/hr	Weight of ingot, lb	Per cent carbon in ingot	Condition of tip
147	400–600	—	½	0.31	Uncoated
152	400–600	2.0	5¾	0.03	Coated
153	400–600	1.7	5½	0.03–0.02	Coated

* Bureau of Mines sponge zirconium used.

TABLE IV. *Results of experiments to determine carbon pickup in titanium sponge from a series of newly coated graphite tips after the first few melts*

Tip	Melt No.	Carbon content of titanium after melting	Carbon pickup*	Brinell hardness
#1	397	0.06	0.025	179
	398	0.038	0.003	163
#2	399	0.07	0.035	185
	400	0.04	0.005	161
#3	401	0.07	0.035	181
	402	0.14	0.105	197
	406	0.05	0.015	170
#4	407	0.04	0.005	192
	408	0.03	0.000	170
#5	409	0.162	0.127	203
	410	0.03	0.000	179
#6	411	0.16	0.125	197
	412	0.03	0.000	165

* Estimate based on the assumption that the sponge before melting contained 0.035% carbon. Three melts with a tungsten tip were found to contain 0.035, 0.030, and 0.042% carbon, respectively, and to have Brinell hardness of 162 to 169.

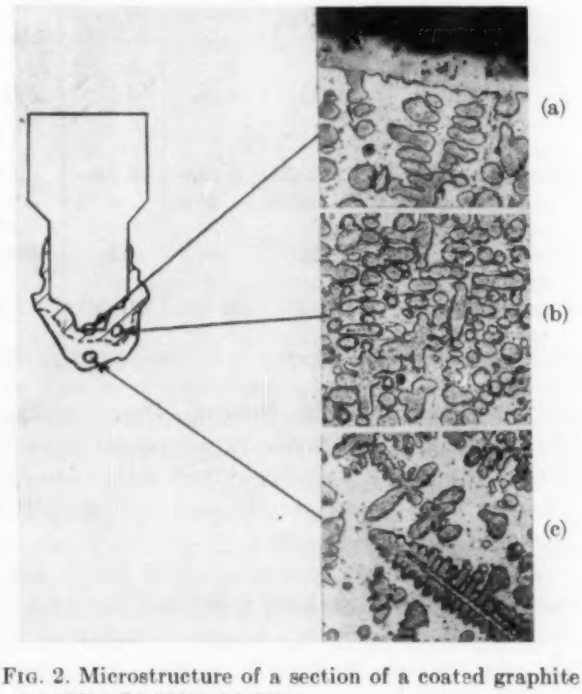

FIG. 2. Microstructure of a section of a coated graphite tip. (a) 100× (b) 100× (c) 100×.

with the exception of the small drop in melting point at the eutectic, the melting point of the Ti-TiC alloys increases with increasing carbon content from about 1800°C to a maximum of about 3150° ± 100° C at 20 per cent carbon for the carbide. Observations of the arc in a special furnace indicate that the surface of the cathode tip surrounding the cathode spot is considerably cooler than the cathode spot itself. This is particularly noticeable for water-cooled electrode tips and at low arc currents. Thus it is reasonable to assume that in the higher ranges of carbide concentrations the titanium-carbide pseudobinary alloys are solid except within and immediately adjacent to the cathode spot.

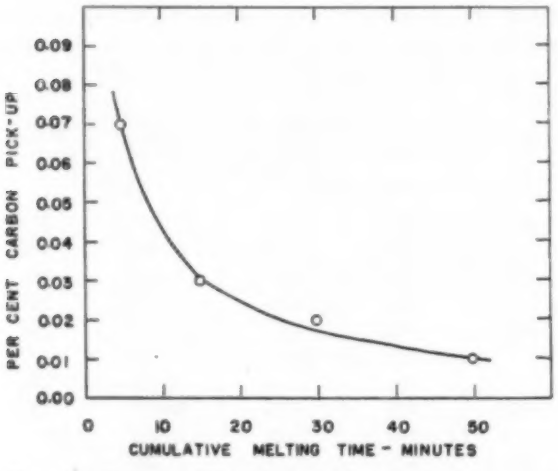

FIG. 3. Curve showing the relation between carbon pickup from a newly-coated graphite tip and cumulative melting time of successive melts of 200 grams using an arc current of 400 amperes.

TABLE V. *Classification of 50 melts made with a specific lot of sponge titanium in a 2¼-inch diameter arc furnace*

	Unacceptable melts			Normal melts
	Excessive carbon by inspection	Operational difficulties	Conditioning melts	
Number of melts	4	3	5	38
Average carbon content after melting, %	0.138	0.037	0.07	0.0352
Range of carbon contents after melting, %	0.092–0.175	0.032–0.040	0.040–0.13	0.015–0.072
Average Brinell hardness	194	188	191	168.4
Range of Brinell hardness	179–204	183–195	177–207	152–184

The titanium on a newly-coated tip is low in carbon and, therefore, has a lower melting point than the coating on a tip that has been in service. Also, the dip-coating technique applies an excessive amount of titanium to the initial tip because the tip is dipped cold. Since low arc currents are used during the initial stages of melting, the temperature of the tip is not great enough to melt the initial excess titanium off. Solution and diffusion of carbon into the titanium coating occurs rather rapidly. When the current is raised for more efficient melting, some of the coating melts and drops off, carrying carbon into the melt. This process gradually ceases as the excess titanium on the tip is removed, and the coating remaining becomes saturated with carbon and hence too refractory to drip off into the melt. The conditioning of the tips is explained in this manner, and the effect is illustrated in Fig. 3, where the progress of conditioning with time is revealed.

Performance of Titanium-Coated Graphite Tips

Data on hardness and carbon content were compiled for a large number of melts made from a specific lot of sponge. In making these melts, both graphite- and tungsten-tipped electrodes were used.

An analysis of data for fifty 120-gram melts made with graphite tips is summarized in Table V. It was found necessary to separate the melts into two groups—melts regarded as acceptable and those not acceptable—for the following reasons: (*a*) melts containing excessive carbon, or over 0.075 per cent; (*b*) melts unacceptable because of known operational difficulties; and (*c*) conditioning melts made with a new tip.

Melts containing excessive carbon could be readily identified by the characteristic appearance exhibited by the anode surface of the buttons. These, without exception, were abnormally hard. When difficulties with the operation of the furnace were experienced, the buttons produced, although low in carbon content, were high in hardness and were generally discolored. Melts made with newly-coated tips were invariably high in hardness and exhibited wide variation in carbon content.

During the period in which the data in Table V were collected, a total of 158 evaluation melts, including the 50 referred to above, were made with titanium sponge of both very good and very bad melting quality. A total of five graphite tips were used for these melts, the life of which varied from 2 to 67 melts per tip. The average life may be regarded as about 32 melts per tip. The life of a tip was determined largely by the melting quality of the sponge. Contamination of the melt by carbon could be expected when there was a heavy accumulation of titanium on the tip. Such tips, however, could be reconditioned for added life. The percentage of melts exhibiting high carbon, or over 0.075 per cent C, was 3.8 per cent. The percentage of melts that were repeated because of operational difficulties was 3.7 per cent.

Comparison of melts made with tungsten tips vs. those made with coated graphite tips.—Fig. 4 (*a*) is a frequency diagram of the distribution of the carbon contents of normal melts made with coated graphite tips. A similar type of distribution, Fig. 4 (*b*), was obtained for melts made with tungsten-tipped electrodes except that this distribution is displaced about 0.01 per cent in the direction of lower carbon content. It is to be noted that both distributions are non-symmetrical, with the preponderance of values toward low carbon contents. The reader is reminded here that these distributions reflect the variations in carbon pickup from the tip, the errors in carbon analysis (±0.01%), and the variation of carbon in each 120-gram sample of sponge melted.

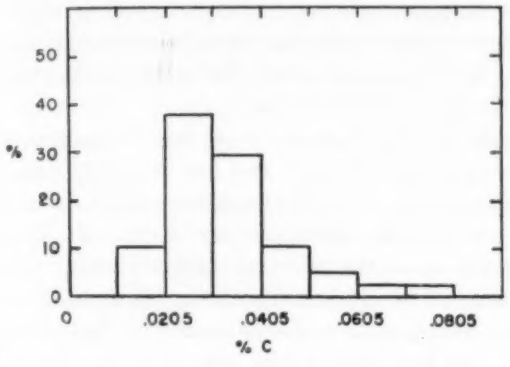

FIG. 4(*a*). Titanium-coated graphite tipped electrode

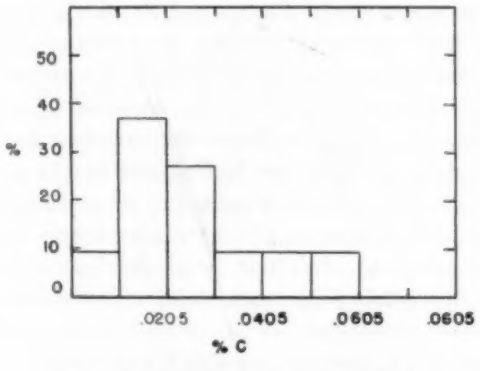

FIG. 4(*b*). Tungsten-tipped electrode

TABLE VI. *Comparison of hardness values and carbon contents of melts made with tungsten and graphite tipped electrodes using a single lot of sponge titanium*

Number of melts, averaged	Type of electrode tip	Average Brinell hardness of melts	Average carbon content of melts
11	Tungsten	169.0	0.0264
38	Graphite	168.4	0.0352

Table VI compares the data for melts made with the two types of tips, tungsten and coated graphite. The average carbon pickup of 0.009 per cent from graphite tips produced no significant increase in the average hardness as compared with buttons made with tungsten-tipped electrodes.

Fig. 5 (*a*) and (*b*) compare the distribution of hardness values of melts made with graphite- and tungsten-tipped electrodes, respectively. Three chief sources of variation account for these distributions—variation in carbon, in oxygen and nitrogen, and errors in hardness measurements.

The use of coated graphite tips produced a normal type distribution whereas that for the tungsten-tipped electrodes is skewed sharply toward high hardness values. Since the carbon distribution for tungsten tips is skewed toward low carbon contents, it was expected that the hardness distribution would be slanted toward lower values. As the reverse was observed, a correlation plot of hardness and carbon content was prepared, as shown in Fig. 6, to test this observation. A slight tendency for the points to cluster along a line of decreasing hardness with increasing carbon contents up to about 0.04 per cent carbon may be noted. This is probably due to the influence of some other factor than carbon content on the hardness.

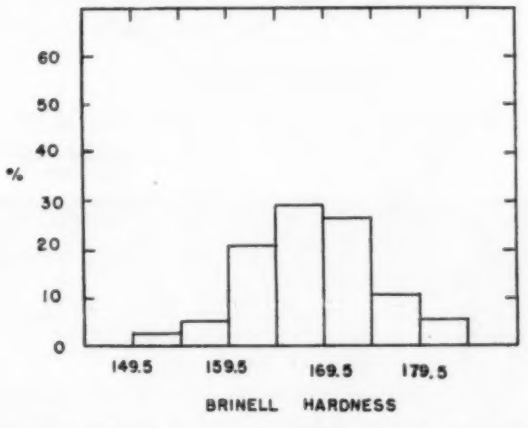

FIG. 5(*a*). Titanium-coated graphite-tipped electrodes

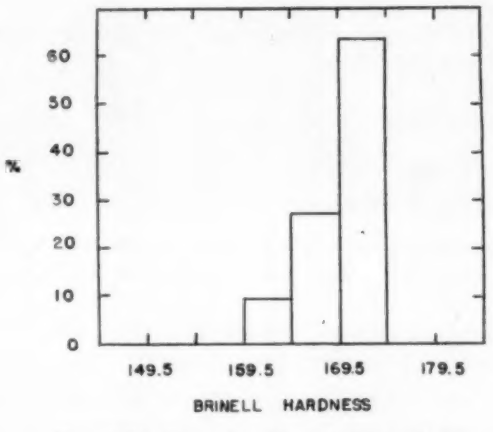

FIG. 5(*b*). Tungsten-tipped electrodes

Effects of Carbon Contents on the Melted Titanium

Analysis of the data for a correlation between carbon contents and macroscopic appearance of the melts indicated that the anode surfaces of melts having about 0.075 per cent carbon and less were characterized by a fine-grained equiaxed structure and a bright silvery anode surface, whereas those having carbon contents greater than this value in-

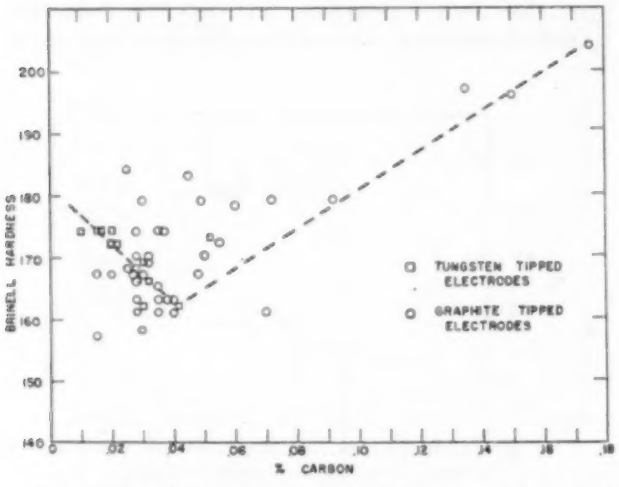

FIG. 6. Correlation plot of Brinell hardness values and carbon of melts made with specified titanium sponge.

TABLE VII. *Results of carbon determinations and hardness tests on the side of a titanium ingot melted with a coated graphite tip* (samples taken every half inch on the surface from top to bottom).

Interval sampled	Distance from top of ingot to middle of interval inches	Brinell hardness at center of each interval	Per cent carbon in turnings from each interval
1	¼	189	0.240
2	¾	152	0.067
3	1¼	146	0.067
4	1¾	146	0.035
5	2¼	143	0.090
6	2¾	143	0.067
7	3¼	134	0.035
8	3¾	133	0.050
9	4¼	146	0.067
10	4¾	131	0.072
11	5¼	143	0.035
12	5¾	150	0.143
Average		146	0.081

variably exhibited a relatively heterogeneous mixture of larger grains and a dull, smooth, matte finish. This sharp difference in surface characteristic provided a reliable qualitative test for separating the high carbon melts from the low carbon melts in evaluation tests, so that a button accidentally contaminated by carbon in melting would be rejected on the basis of its surface appearance and not assumed to represent properly the sponge from which it was made.

Metallographic examination of low-carbon buttons showed the acicular structure of transformed beta. The high carbon melts containing over 0.075 per cent carbon showed rounded particles of TiC in a matrix of transformed beta. These observations are in substantial agreement with the constitution diagram of titanium and carbon presented by Jaffee, Ogden, and Maykuth (2). The presence of the large grains in the high carbon melts cooled through the beta + TiC field, as compared to the finer grained structure of the low carbon melts cooled through the beta titanium field, cannot be adequately explained. It appears, however, that their presence is closely related to the appearance of TiC in the microstructure of titanium-carbon alloys.

Melts having high hardness due to contamination by oxygen and nitrogen and less than 0.075 per cent carbon exhibited much the same surface structure as the low carbon alloys already described. This was expected since the effect of oxygen and nitrogen in the amounts compatible with the hardness values of our titanium-carbon alloys is simply that of raising both the beta and alpha solvus lines. No second phase was formed as with titanium containing greater than 0.075 per cent C.

From the work of Finlay and Snyder (3), carbon up to 0.075 per cent produces an increase in hardness amounting to about 3.3 Brinell points for every 0.01 per cent carbon added to titanium. Thus the maximum hardness increase corresponding to a carbon pickup of 0.075 per cent could not be greater than about 25 Brinell points, and no important increase in hardness due to carbon pickup from a coated graphite electrode need be feared in the titanium melted with such an electrode, if the tip and other conditions are adjusted to give a carbon content in the melt below 0.075 per cent.

Current Capacity of Graphite Tips

Experiments were conducted to determine the maximum current that can be used with coated graphite electrode tips without obtaining excessive carbon pickup.

A series of 150 to 200 gram melts was made in a 2½-inch diameter arc furnace using progressively higher currents. The graphite tip shown in Fig. 1 was used. The indications were that currents as great as 1000 amperes could be used with carbon pickup of 0.05 to 0.07 per cent.

On the basis of these results, a 6-pound ingot was made in a 3-inch diameter arc furnace using an arc current of 900 to 1000 amperes at an arc voltage of 30. A tip of the design shown in Fig. 1 was used. Carbon determinations on lathe turnings taken at regular intervals along the side of the ingot give some idea of the carbon distribution (see Table VII). The

tip was shortened by about ¼ inch after melting, but still retained its Ti-TiC coating.

Although the average values of carbon content and hardness are low, the variation in both these values is such as to indicate lack of homogeneity with respect to carbon. It has not been determined whether this degree of inhomogeneity is detrimental in the finished product after working by forging or rolling.

It is believed that the high carbon layers in the ingot were caused by sudden melting off of accumulations of titanium-carbon alloy, resulting from titanium spattering on the electrode during melting. The use of a spatter-free sponge would probably help to reduce the inhomogeneity caused by carbon, as well as that caused by tungsten, in arc-melted titanium ingots.

Use of large graphite tips for heavy currents. —Larger graphite tips were designed for currents heavier than 1000 amperes. Two tips were designed, one a 1½-inch diameter tip, and the other a 2-inch diameter tip. Both were fitted to water-cooled copper electrodes.

In tests conducted with the 1½-inch tip, the titanium-TIC coating melted off. However, it was noted in these experiments that the faster melting times produced the ingots having the lowest carbon content. As yet the 2-inch tip has not been tested.

Since in these tests with currents greater than 1000 amperes enough heat was generated at the cathode spot to melt the titanium-TiC coating on the entire surface of the tip, so that the coating then dropped off or was blown off by the arc blast, a solution of the problem of developing a tip to withstand these conditions seems to involve one or more of the following expedients:

1. Increasing the intensity of cooling so as to limit the volume of molten materials to the immediate vicinity of cathode spot. This may be accomplished by increasing the cross-sectional area of the tip and shortening the length of the tip.

2. Use of a coating metal that forms a carbide of higher melting point, so that the volume of molten metal in the vicinity of the cathode spot will be substantially reduced.

3. Using magnetic or other means to cause the cathode spot to travel over the surface of the tip at such a rate as to prevent conditions of maximum heating at the cathode spot. This would increase the area of the cathode spot and prevent excessive heating of localized areas of the tip. This is analogous to the rotating anodes used in certain high intensity x-ray tubes. The disadvantage of this method is that movement of the cathode spot will probably result in rapid movement of the anode spot and reduce the penetrating power of the arc on the melt. However, the increased current carrying capacity might more than compensate for this deficiency. Considerable additional work is required on this problem.

Heat Losses in the Inert Atmosphere Arc Furnace

This section deals with a calorimetric study of the heat losses in the water-cooled electrode, crucible walls, and crucible bottom of the inert-atmosphere arc furnace.

The effects of varying arc length, arc current, and arc voltage were investigated to obtain a clearer conception of the actual behavior of the arc during melting, and to provide data useful for the design and operation of new furnaces.

Testing Procedure

The furnace used in these experiments has been described (4).

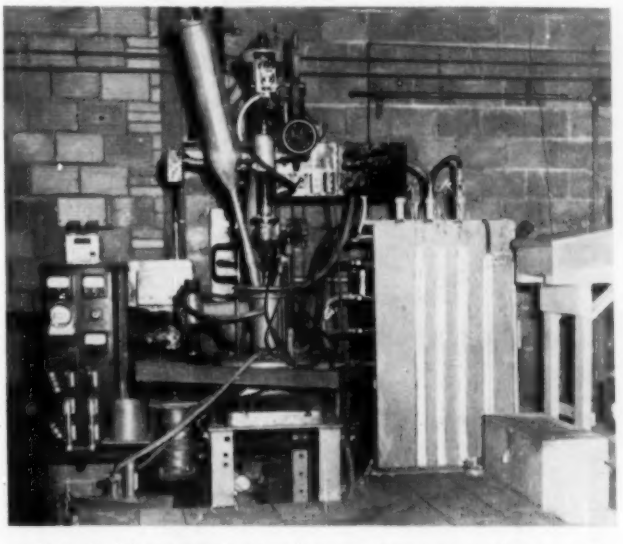

Fig. 7. Photograph showing arc furnace equipment for 3-inch and 5-inch diameter water-cooled crucibles.

The arrangement of the furnace and apparatus for making the calorimetric measurements is shown in Fig. 7. The flow gauges were calibrated *before* each series of experiments. Inlet and outlet water temperatures were carefully measured during the tests. Arc lengths were taken as the distance between the lowest extremity of the electrode and the anode surface of the melt. The actual arc length is probably slightly greater than reported, as occasionally the arc would move to a position somewhere between the center and the outside edge of the ingot. The possible maximum error in arc length may range from 80 per cent for a ½-inch arc to 10 per cent for a 2-inch arc length. During the tests, precautions were taken to take all readings of voltage, current, etc., when the arc was at its steadiest and nearest axial position. This was indicated by the lowest and steadiest value of arc voltage and hence gave the smallest error in readings.

Heat Losses

Heat losses to electrodes.—Increasing arc current as shown by the curves in Fig. 8 results in a proportional increase in the heat lost to the cooling water of the electrode. Electrode losses were independent of arc length.

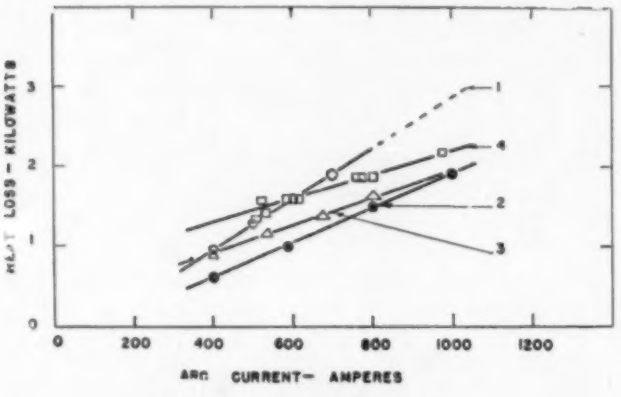

FIG. 8. Electrode heat losses

Curve No.	Slope of curve in watts per ampere	Tip material
1	3.10	Graphite
2	2.16	Graphite
3	1.75	Graphite
4	1.50	Tungsten

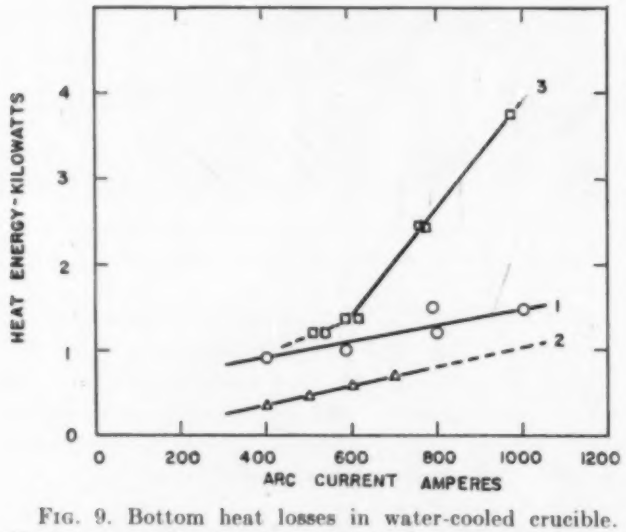

FIG. 9. Bottom heat losses in water-cooled crucible. Curve 1—graphite tip, ingot height 1 inch, curve 2—graphite tip, ingot height, 3 inches, curve 3—tungsten tip, ingot height, 1 inch.

It follows from the two assumptions: (*a*) that the area of the cathode spot is proportional to the current and (*b*) that the temperature of the cathode spot remains constant with increasing arc current (5), and application of the laws of simple heat transfer through a long solid cylinder that

$$Q = BI$$

where Q is the heat energy removed by the cooling water in watts, I is the current in amperes, B is a constant and equal to the slope of the straight line defined by the above expression. It may be expressed in watts per ampere.

The experimental curves are straight lines but, when extrapolated to zero arc current, are found to intersect the ordinate at finite values of heat loss. The empirical relation

$$Q = BI + C,$$

where C is the value of heat loss intercepted at zero arc current by the extrapolated curve, best represents the curves in Fig. 8 at currents greater than 400 amperes.

It is unlikely that the linear relation for arc current and electrode heat loss will hold with currents lower than 400 amperes. Factors which affect heat transfer and arc characteristics, but which exert little influence on heat losses at the high currents, probably increase in importance as the current decreases and would cause increasing deviation from a straight line relation.

Curves 1, 2, and 3 in Fig. 8 are for coated graphite tips of the design shown in Fig. 1.

The variation in the slopes of the curves cannot be fully explained but is probably the result of variations in thermal and electrical conductivity of the tips and contact with the copper electrode. Although the tungsten tip had the best thermal and electrical contact with the electrode, and the smallest value of B (1.50 watts/amp) this does not necessarily imply that the actual heat losses for a tungsten tip should be the lowest, for other factors affecting cathode spot temperatures, etc., must be considered. For example, if the cathode drop or space charge in front of the cathode is higher for tungsten than for the coated graphite tips, the heat released in the immediate vicinity of the tip will be greater for the former than the latter and cause corresponding differences in the heat losses. Also temperature differences between the two cathode spots would likewise influence the comparative heat losses.

Bottom heat losses.—The effects of increasing current on bottom losses using both graphite- and tungsten-tipped electrodes are shown in Fig. 9. Curves 1 and 2 were obtained with graphite tips, making ingots 3 inches in diameter, and 1 inch and 3 inches in height, respectively. Comparison of these two curves gives some idea of the effect of increasing height on the ingot on the amount of heat energy dissipated into the bottom plate. Curve 3 represents the heat energy dissipated into the cooling water of the bottom plate when a tungsten-tipped electrode is used. This curve may be compared with curve 1, the ingot size being the same in both these experiments.

The sudden break that occurs in curve 3 at 600 amperes is evidence of the greater penetration of tungsten arcs. With over 600 amperes and a tungsten tip, the button or ingot must be molten to a greater depth than with a graphite tip.

Heat losses in walls of water-cooled copper crucible.—Characteristic curves of the heat dissipated in the water-cooled copper crucible walls under steady-state conditions are given in Fig. 10. Both increasing current and increasing arc length increase the heat losses in the crucible. In Fig. 11 a similar set of curves is obtained for the electrical power input plotted against arc length for different levels of arc current.

The heat losses in the walls of the water-cooled

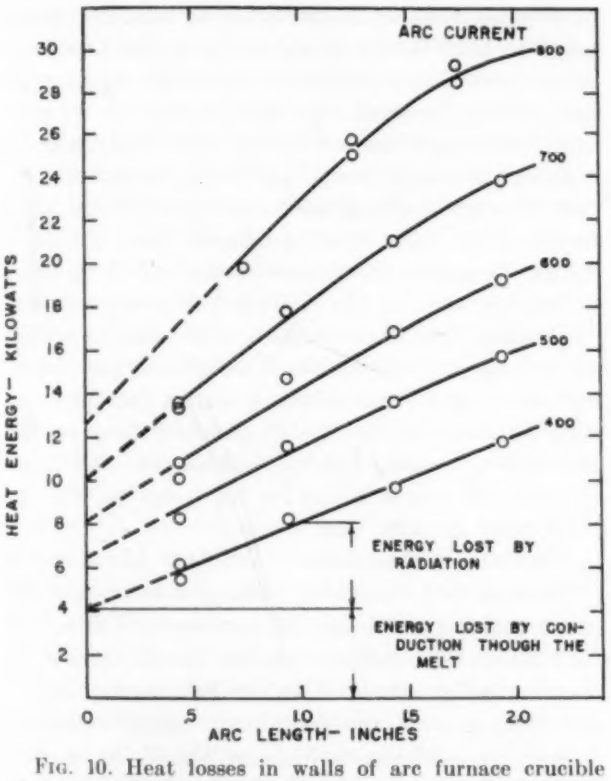

FIG. 10. Heat losses in walls of arc furnace crucible plotted against arc length at various levels of current.

crucible may be divided into two parts: (*a*) that which is transferred directly from the arc to the walls of the crucible, and (*b*) that which is transferred indirectly to the crucible walls by conduction through the ingot. As the arc is shortened, the amount of heat transferred directly from the arc to the furnace walls becomes less until finally at zero arc length this loss may be regarded as being negligible. This is shown in Fig. 10, where the characteristic curves have been extrapolated to intersect the ordinate at zero arc length. The heat loss at zero arc length represents the energy lost to the crucible walls by conduction through the material melted.

A measure of the heat used for melting is provided by the sum of the heat losses in the crucible bottom and in the walls at zero arc length, because the energy lost in these ways has served to heat the metal melted in the furnace before it appeared in the form of losses. This sum, expressed as a percentage of the total power consumed, provides a measure of the efficiency of the furnace. Such percentages have been calculated and plotted against arc length at different

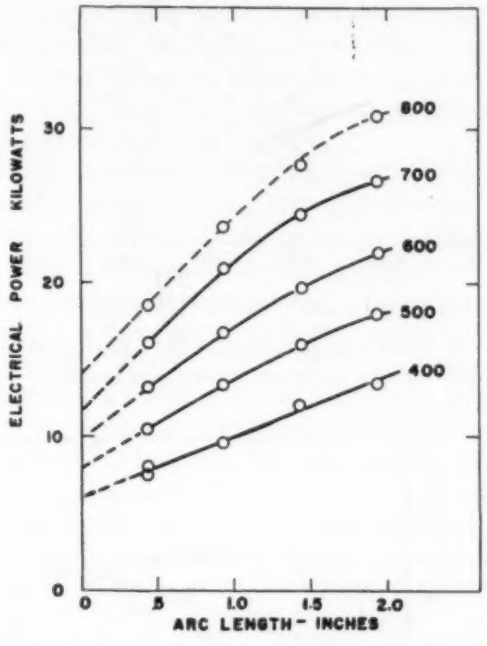

FIG. 11. Electrical power input vs. arc length at various levels of current.

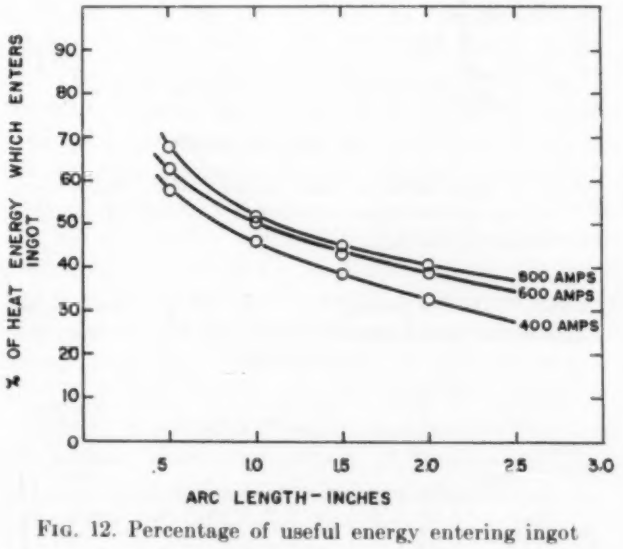

FIG. 12. Percentage of useful energy entering ingot

levels of current in Fig. 12. It is to be noted that most efficient operation is obtained under conditions of high current and short arc lengths.

From the data contained in Fig. 10 curves of the heat energy extracted by the water-cooled crucible walls have been plotted against arc current at different levels of arc length in Fig. 13. The curve for

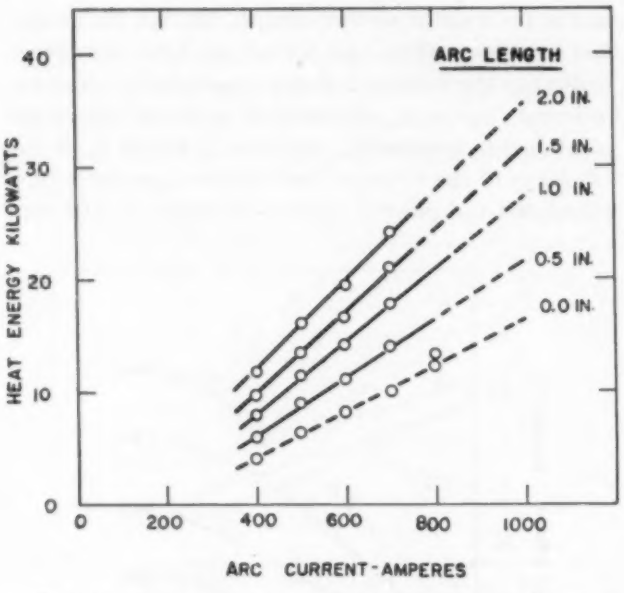

FIG. 13. Heat energy extracted by water-cooled copper walls of furnace for different levels of arc length.

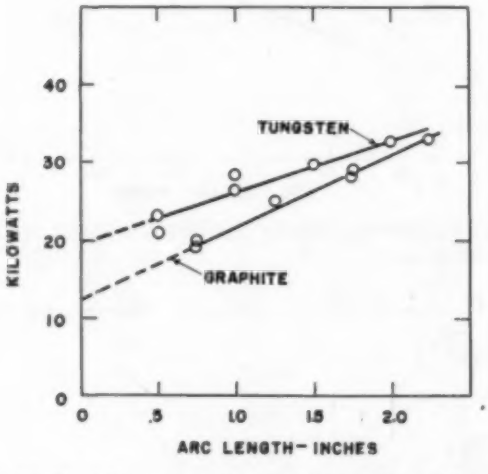

FIG. 14. Heat losses in water-cocled crucible walls. Tungsten- and graphite-tipped electrodes. Current 800 amperes, ingot height 3 inches.

TABLE VIII. *Arc furnace heat losses using graphite-tipped electrode and an arc length of 1 inch to melt a titanium ingot 3 inches high*

Current amp.	Electrical power input (1) kw	Electrode loss (2)		Crucible wall losses (3)		Crucible bottom loss (4)		Heat losses through the melt, or energy entering the ingot (5)	
		kw	%	kw	%	kw	%	kw	%
400	10.0	0.95	9.5	8.0	80.0	0.35	3.5	4.6	46.0
600	16.5	1.6	9.7	14.2	86.0	0.60	3.6	8.2	50.0
800	24.3	2.2	9.0	20.8	85.6	0.80	3.3	12.6	52.0

(1) From Fig. 11.
(2) From Fig. 8, curve 1.
(3) From Fig. 13.
(4) From Fig. 9, curve 2.
(5) From Fig. 12.

zero arc length is most important since it represents the energy lost through the metal that was melted.

Most of the heat transfer from ingot to crucible occurs at the surface of the crucible in contact with liquid metal, although some of this transfer occurs also through a solid titanium-gas-copper interface between the solidified part of the ingot and the copper walls. A gas gap, formed by contraction of the freezing metal, separates the ingot from the copper walls, so that the greater loss occurs from the melt which is in contact with the copper.

Comparison of heat losses in walls with tungsten- vs. titanium-tipped graphite electrode.—Visual observation of arcs produced by graphite- and tungsten-tipped electrodes indicated that tungsten produced a more penetrating or intense arc than titanium-coated graphite did. Thus a tungsten tip should produce a deeper pool of molten metal at the top of the ingot and thereby increase the area of contact between liquid metal and water-cooled copper. Consequently, a given amount of energy produced through a tungsten arc should give greater losses through the ingot to the walls than those produced from the same energy through a titanium-coated graphite tip. This is demonstrated by the characteristic curves in Fig. 14 in which heat losses in the crucible wall have been plotted against arc length. The heat energy loss at zero arc length is considerably higher for the tungsten tip than for the coated graphite tip, and the proportion of energy lost by radiation and convection per unit arc length is less for the tungsten than for the coated graphite tips.

Summary of heat losses.—The heat losses in the graphite-tipped electrode, walls, and bottom of the water-cooled crucible are summarized in Table VIII for a 3-inch diameter arc furnace. These results show that increasing current does not have a very important influence on the percentage losses measured. Larger single electrode furnaces should have comparable losses, but with a somewhat higher percentage of useful energy due to the greater ratio of volume of metal to surface area of ingot. Multiple electrodes should result in an additional increase in efficiency. Most efficient operation should be obtained with consumable electrodes because the short arc would minimize direct radiation losses, and the heat developed in the electrode would be utilized for melting. The losses summarized above do not include the sensible heat in the ingot. This constitutes the largest body of stored heat in the system, other stored heat being insignificant in comparison. A small fraction of the radiant heat from the arc and surface of the melt lost through the cover of the furnace is not accounted for by the heat losses measured in the water-cooled crucible. These losses result in slightly

lower overall melting efficiency than has been estimated.

The overall melting efficiency suffers an additional drop during operation of the furnace due to accidental delays and the relatively short intermittent delays which occur during charging of the sponge. During these periods metal is not being melted, and the heat is lost wastefully through the water-cooled walls of the furnace. Also, heat is spent in driving off volatile impurities in the sponge. It becomes more or less apparent then that the 40 or 50 per cent of the total power input that was shown to enter the ingot during steady-state conditions may actually undergo wide fluctuations during melting depending upon the quantity of sponge being melted at a given instant.

Several factors operate to improve the melting efficiency. One very important one is the fact that the porous sponge, due to its low heat conductivity and poor contact with the crucible walls and ingot, becomes heated rapidly to the melting point before the heat has an opportunity to dissipate wastefully. As the loose charge of sponge becomes consolidated by fusion, the percentage of heat entering the ingot approaches the values that were obtained under steady-state conditions.

If an accurate heat balance could be made of all the possible heat losses in the dynamic system, it is estimated that values would be arrived at not differing too greatly from the values obtained under steady-state conditions, perhaps tending to the low side.

From the above discussion, it becomes clear that the operating practice, including the manner of charging the sponge, manipulation of the electrodes, (manually or mechanically), the arc length, etc., has a major influence on the overall melting efficiency.

It has been indicated by the data reported that at constant arc current the power increase resulting from increasing the arc voltage by lengthening the arc is lost directly through the walls of the crucible and results in a loss in melting efficiency. However, the results with a higher voltage arc produced by the tungsten-tipped electrode, as compared to those with a graphite-tipped electrode suggest that the efficiency of the arc furnace might be improved by using gases or electrode materials which produce higher voltage arcs.

Conclusions

1. Cathodic electrodes of ¾-inch diameter, provided with graphite tips coated with a titanium-carbon alloy, may be employed for melting sponge titanium in an inert-atmosphere arc furnace without excessive carbon pickup, provided the current used is not over 1000 amperes. Out of 158 melts made with such coated graphite electrodes, only 3.8 contained over 0.075 per cent carbon.

2. Comparing carbon pickup using coated graphite tips with that using tungsten tips, it was found that the average excess pickup with the former practice over that with the latter was only 0.01 per cent, and that this amount of carbon produced no significant increase in the average hardness of the melts.

3. The average number of melts that may be made with a ¾-inch diameter coated graphite tip using less than 1000 amperes is about 32 and may range from 2 to 67 before the tip is rendered useless by mechanical failure or excessive accumulation of titanium-carbon alloy. The life of a tip depends largely upon the melting quality of the sponge.

4. Larger uncoated graphite electrode tips may be used with currents higher than 1000 amperes, but comparatively large amounts of carbon are then introduced into the melts. Carbon pickup with such tips may be controlled, by careful restriction of arc current and melting rate, to values between 0.20 and 0.30 per cent carbon.

5. Arc melts containing 0.075 per cent or more carbon may be readily identified and separated from melts containing less than this amount by the characteristic appearance exhibited by the anode surface of the metal after solidification. This provides a reliable qualitative control test for separating high and low carbon melts in evaluation testing of titanium sponge.

6. Electrode heat losses may be represented at currents greater than 400 amperes by a straight line equation: $Q = BI/1000 + C$ where Q is the heat loss in the electrode in kilowatts, I is the current in amperes, and B and C are constants for a given electrode. For different electrodes the value of C decreases with increasing values of B. In the work reported, C varied from $+0.7$ for a value of $B = 1.5$ watts per ampere to -0.3 for a value of $B = 3.1$ watts per ampere.

7. By plotting the arc length against the heat absorbed in the walls of the inert-atmosphere arc furnace for a given current, and extrapolating the curve to zero arc length, a value of the heat lost to the walls through the metal melted is obtained; and this value added to the heat lost through the furnace bottom provides a measure of the energy utilized in heating and melting the metal charge. By comparing this with the total input of energy, the efficiency of the furnace for the given current is arrived at. With 1-inch arc length and 600 amperes current, this efficiency was about 50 per cent.

8. At constant current, the power increase resulting from increasing the arc voltage by lengthening the arc is almost entirely lost directly to the walls of the water-cooled copper crucible and results in a loss in melting efficiency.

9. Tungsten-tipped electrodes are considerably

more efficient for melting titanium than coated graphite tips for the same current and arc length.

10. Increasing arc current does not have a very important influence on the percentage heat losses in the electrode, crucible walls, or bottom of the arc furnace for a given arc length under steady-state conditions. These losses amounted to approximately 10, 84, and 3.5 per cent, respectively, with graphite-tipped electrodes, the remainder being largely accounted for by resistance losses. The sensible heat of the ingot, and radiation through the cover, are comparatively unimportant causes of heat loss.

Acknowledgment

The author wishes to express his appreciation to the management of the Titanium Alloy Manufacturing Division of the National Lead Company for permission to publish the results of this investigation. The counsels and criticisms of Dr. S. F. Urban, Director of Research, and Mr. R. S. Stewart, Assistant Chief of the Physical Metallurgy Division, have been invaluable to the author. Particular thanks are due to Mr. E. Johnson, who gave most valuable help to the author throughout the investigation.

Any discussion of this paper will appear in a Discussion Section, to be published in the December 1952 issue of the JOURNAL.

REFERENCES

1. "Titanium, Report of Symposium, December 16, 1948," p. 155, sponsored by Office of Naval Research, Department of the Navy, Washington, D. C.
2. R.I. JAFFEE, H. R. OGDEN, AND D. J. MAYKUTH, *Trans. Am. Inst. Mining Met. Engrs.* (*J. Metals*), **188,** 1261 (1950).
3. W. L. FINLAY AND J. A. SNYDER, *Trans. Am. Inst. Mining Met. Engrs.* (*J. Metals*), **188,** 277 (1950).
4. W. E. KUHN, *J. Electrochem. Soc.*, **99,** 89 (1952).
5. W. SPRARAGEN AND BELA A. LENGYEL, *J. Am. Welding Soc., Research Suppl.*, **8,** 13s (1943).

The Relationship of Alpha and Beta Silicon Carbide[1]

HENRY N. BAUMANN, JR.

Research and Development Division, The Carborundum Company, Niagara Falls, New York

ABSTRACT

Silicon carbide was formed under various time-temperature conditions from mixtures of silica and carbon and of silicon and carbon. The products were examined by x-ray diffraction, electron and optical microscopy, and chemical analysis. It was found that (*a*) primary silicon carbide, which is always beta SiC, could be formed as low as 525°C when carbon and silicon were contained in a low melting alloy of aluminum and zinc; (*b*) beta SiC is stable to near 2100°C; (*c*) under certain experimental conditions beta SiC showed no significant crystal growth when held for 44 hours at 1400°C and only small growth (microscopic) up to 2100°C; and (*d*) that the change from beta to alpha silicon carbide is monotropic, and is complete after a few minutes at 2300°C.

INTRODUCTION

The crystal structures and related physical properties of the different forms of silicon carbide have been well established in recent years, and the structural relationship of the two distinct crystalline species, alpha and beta silicon carbide, are satisfactorily described by Thibault (1), Ramsdell (2), and Kohn (3). The chemical and time-temperature relationships of these two species have not been so clearly demonstrated, and it is the purpose of this paper to present experimental data and observations that contribute toward the solution of that problem.

A cubic form of silicon carbide in addition to the three hexagonal system types then known was discovered by Ott (4) in 1926. This material obtained from the German Carborundum Company was commonly called "amorphous silicon carbide," and consisted of loose lumps of a fine gray powder that gave a greenish streak. It is always found near the outer section of commercial silicon carbide furnaces. Chemically, it closely approximated the composition SiC. The nature of this material, according to Ott, could only be determined by powder x-ray diffraction analysis. The new pattern contained most of the strong lines of the previously known hexagonal variety, but was that of a cubic crystal whose unit cell was of the diamond type.

The Crystallography of Silicon Carbide

For the purpose of the present study it is necessary to review only briefly the crystallography of silicon carbide. Thibault (1) proposed that cubic silicon carbide be named beta SiC, and that the hexagonal varieties that occur in both the rhombohedral and hexagonal divisions of the hexagonal system be grouped as alpha SiC. Lundquist (5) objected to this nomenclature as not conforming to phase diagram practice. Neither phase rule practice nor mineralogical nomenclature are very consistent in this regard, and Thibault's nomenclature has proved so convenient that crystallographers and mineralogists have generally accepted it.

Alpha SiC occurs in at least ten different crystalline forms so closely and peculiarly related structurally that they are now called types, rather than modifications. Of these, only three are of common occurrence, and one type constitutes the bulk of commercial silicon carbide. This latter type that had been called Modification II by Baumhauer (6), who first discovered it by goniometry, is now designated as Type 6H Alpha SiC in Ramsdell's (2) system of classifying silicon carbide crystals.

That beta SiC along with many other finely crystalline materials should have been considered amorphous prior to the discovery of x-ray diffraction methods of crystal examination is obvious. This is particularly true of beta SiC which is optically isotropic when particles large enough to examine microscopically are observed under crossed nicols in the petrographic microscope. However, occasional crystals of octahedral habit with some developed faces have been found and examined goniometrically and by Laue and rotation x-ray techniques. The first report of such a study was by Braekken (7), who worked with a single octahedral crystal whose greatest dimension was 0.5 mm. This is about the maximum size crystal to be found, and even crystals of this size are almost always anhedral, that is, without any developed crystal faces.

The Chemistry of Silicon Carbide Formation

In considering the relationship of alpha and beta SiC, the problem resolved itself first into a study of the formation of silicon carbide under different time-temperature conditions. Commercially, silicon carbide is always manufactured from a mixture of silica

[1] Manuscript received August 28, 1951. This paper prepared for delivery before the Washington Meeting, April 8 to 12, 1951.

sand and some form of carbon low in ash. The chemical reaction is generally represented as:

$$SiO_2 + 3C = SiC + 2CO.$$

Previous workers studied this reaction in small laboratory furnace experiments. The most systematic published work along these lines was that of Ruff (8) and his coworkers who concluded that the reaction begins above 1500°C, and, under the condition of his type of experiment, is complete at 1800° C. In the present work numerous experiments were made involving this reaction under different time-temperature conditions. The reaction:

$$Si + C = SiC$$

was carried out in similar time-temperature experiments. The latter is not only of theoretical interest, but is the basis of manufacturing a form of siliconized silicon carbide described by Rose (9).

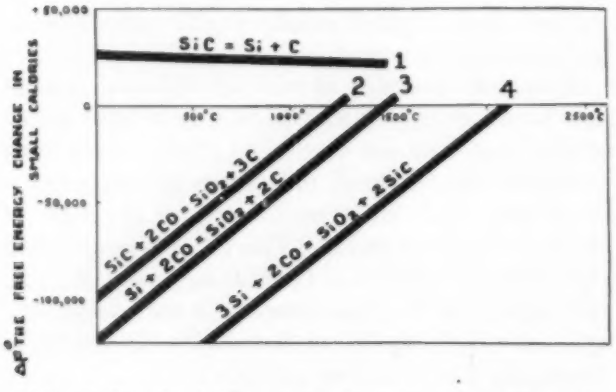

FIG. 1. Standard free energy change vs. temperature for reactions pertinent to the formation of silicon carbide.

A series of experiments to cover the time-temperature range required to solve the problem were outlined on the basis of the thermodynamic data calculated by Read (10) (see Fig. 1). All experiments were performed at atmospheric pressure.

While thermodynamic equilibrium generally does not exist under conditions such as are found in commercial silicon carbide furnaces, these calculations are still useful in choosing one or more of several possible reaction mechanisms that may take place. For example, the reaction Si + C = SiC is thermodynamically feasible even at room temperature. Also, the curves tell us nothing regarding such properties as rates of reaction, but by placing limits to which various reactions may proceed, they furnish valuable guides for both outlining and observing experimental work.

Description of Experiments

Several types of furnaces were used. In a preliminary series involving both reactions named above, mixes of silica and carbon, and of silicon and carbon, each of good technical quality, were introduced into graphite cylindrical "bombs" 4 inches long and 3 inches in diameter. In one end of each of these bombs a hole one inch in diameter and 2½ inches deep was bored. The mix was placed into this hole and the opening was plugged with a tight-fitting graphite rod. The bombs were coated with a refractory high alumina cement to minimize oxidation of the outer surface. The reaction mixes were heated to different temperatures up to 1800°C at which they were held for definite periods of time in oil-fired kilns. For runs at 1400°C or less, an electrical resistance furnace equipped with Globar silicon carbide heating elements was used.

A hollow graphite tube resistance furnace was used for preliminary experiments in the temperature range 1800° to 2400°C, mix being contained in graphite boats, and the temperature measured by optical pyrometry. Its design and operation was similar to the high temperature tube furnace described by Gartland (11).

A third type of furnace used for both preliminary experiments and the later more quantitative experiments was the Ajax-Northrup high frequency furnace. In these, the experimental mixes were contained in covered graphite crucibles. At intervals over a period of years, different experiments designed to test out various theoretical ideas were made in these furnaces. On the basis of the results of these preliminary runs, more recent experiments capable of a more quantitative interpretation were made.

The Preliminary Experiments

Table I summarizes some of the more pertinent results of the first experiments.

Electron Microscopy

To illustrate the results of the study of crystal growth by electron microscopy, micrographs made on a Model EMB-4 RCA electron microscope are shown. The samples were mounted on nitrocellulose film. Fig. 2 from the reaction Si + C = SiC at 1400°C, one hour run, shows aggregates of equant particles on the order of one micron and less in diameter, only a few of the particles being completely dispersed. Other micrographs up to 44 hours were similar to Fig. 2, no crystal growth being evident. The same reaction held one-half hour at 1600°C showed only slight crystal growth. Fig. 3, for the reaction SiO_2 + 3C = SiC + 2CO for one-half hour at 1750°C, indicates crystal size on the same order as Fig. 2 except for the few larger skeletal crystals. When held at 1750°C for 28 hours some crystal growth took place, but the particles are still skeletal and microcrystalline. There was no marked crystal growth until above

TABLE I

Note: The products of the experiments recorded herewith were examined by the x-ray powder diffraction method in order to detect presence of silicon carbide, and in some cases electron micrographs were made in order to study crystal growth, etc. HF denotes high frequency furnace.

PART I. *Experiments involving reaction* Si + C = SiC, *both bomb type and high frequency furnace runs*

No.	Description	Results and observations
1	Reaction mix Silicon (97% grade) 70% Carbon (99% grade) 30% 1. 5 hr 1365°C 2. " " 1425 3. " " 1500 4. " " 1800	All products contained microcrystalline beta SiC, but No. 1 had residual Si.
2	Silicon (90% grade) 70% Carbon (99% grade) 30% 5 hr at 1200°C	Produced small amount of microcrystalline beta SiC, and considerable residual silicon.
3	Silicon (99+% grade) 70% Carbon (99% grade) 30% 1 hr at 1300°C 1 hr at 1400° C	1300°C run has a loose product free of SiC; 1400° C contained considerable beta SiC.
4	Carbon 10% Equal parts Aluminum and silicon 90% 1 hr at 1000°C	Beta SiC, and residual aluminum and silicon.
5	Carbon (99% grade) 6% Silicon-nickel eutectic (Si 38 parts, Ni 62 parts) 94% 1 hr at 1000°C	Beta SiC, nickel, minor amounts of silicon.
6	Carbon 6.7% Silicon 13.3 Aluminum 26.7 Zinc 53.3 3 hr at 525°C	Beta SiC present in small amount in residual Al, Zn, and Si. After treating with hydrochloric acid the greenish gray residue gave a strong x-ray diffraction pattern for SiC.
7	Si + C = SiC held at 1400°C and samples withdrawn periodically. A1—½ hr 2—3 " 3—6 " 4—12 " 5—20 " 6—28 " 7—36 " 8—44 "	All beta SiC—sub-microscopic. Electron micrographs showed no crystal growth.

2100°C, when x-ray diffraction analysis indicated the first development of the alpha SiC crystalline phase.

THE QUANTITATIVE EXPERIMENTS

The previously described experiments give a fair picture of the formation of primary silicon carbide which is always of the beta SiC species. On the basis

PART II. *Experiments involving reaction* $SiO_2 + 3C = SiC + 2CO$

No.	Description	Results and observations
8	A series of bombs and HF runs using SiO_2 (99+% grade) Carbon (99+% grade) 7 runs from 1500° to 2000°C Each held 1 hr	1500°C—no SiC, but graphite, quartz, and cristobalite. 1635°C—similar to 1500°C, some beta SiC. 1700°C—beta SiC 1800°C—beta SiC 2000°C—green isotropic microcrystalline particles—beta SiC x-ray pattern.
9	Carbon with prefused CaO-SiO_2 eutectic melting at 1436°C 1 hr at 1450°C	Small amount of beta SiC—considerable residual wollastonite.
10	A number of HF and tube runs—at temperatures in the 2200°–2400°C using Ottawa sand and different sources of carbon.	Experiments held at 2250°C for 20 minutes produced fine green anisotropic alpha SiC.
11	$SiO_2 + 3C = SiC + 2CO$ B1—½ hr at 1750°–1800°C 2—3 hr 3—6 " 4—12 " 5—20 " 6—26 " 7—36 "	All beta SiC. All submicroscopic. Electron micrographs showed slight crystal growth—but only skeletal crystals submicroscopic to microcrystalline.

of these experiments, two more series were carried out in the high frequency furnace. With the aid of a North American Phillips x-ray spectrometer, it was possible to obtain quantitative data showing the relative amounts of beta and alpha SiC. The calibration data were derived by determining the ratio of the amplitudes of the 2.51 Å line common to beta and alpha SiC with that of the 2.36 Å line of 6H alpha SiC. The first series of experiments consisted of a set of mixes of SiO_2 and carbon, and a set of Si and carbon. The silica was from crushed clear quartz crystal, the silicon chemically pure material from the Electro-Metallurgical Company, and the carbon from spectrographic quality graphite electrodes. The aluminum content of the silicon-carbon reaction varied from 0.15 to 0.03 per cent, in the silica-carbon runs 0.06 to 0.03 per cent. The maximum iron percentage run was 0.13, the minimum 0.01. The products were, therefore, exceptionally pure.

The experiments were run in covered graphite crucibles that were prefired to the temperature of each run. They were then run in pairs, one containing the mix, the other employed as a control.

Fig. 4 summarizes graphically the chemical results of the first two sets of experiments. In order to compare the two types of reactions, the percentages SiC conversion are calculated on the basis of silicon in the products and in the original mixes. It is worth noting

that the carbon monoxide of the furnace acts as an oxidizing agent at certain temperatures in the silicon-carbon reaction. While the silicon-carbon reaction

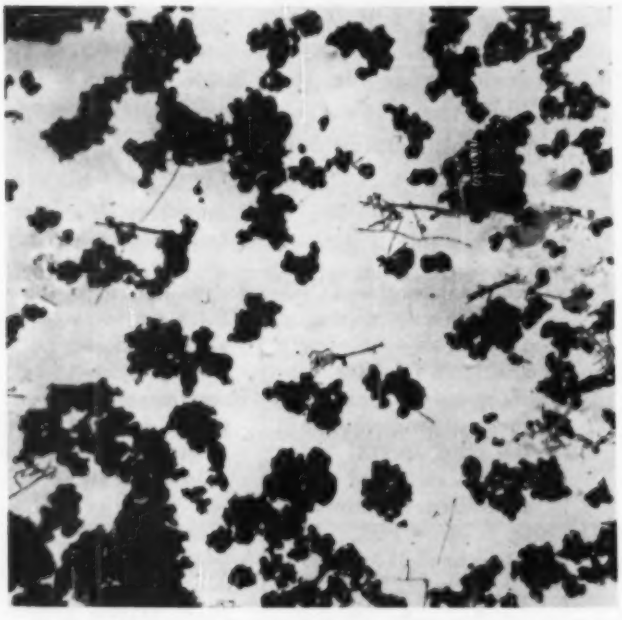

FIG. 2. Electron micrograph. Product of the reaction Si + C = SiC at 1400°C for one hour. All electron microscope samples were heated to eliminate free carbon, and treated with hydrofluoric acid to remove residual silica. 9,000×.

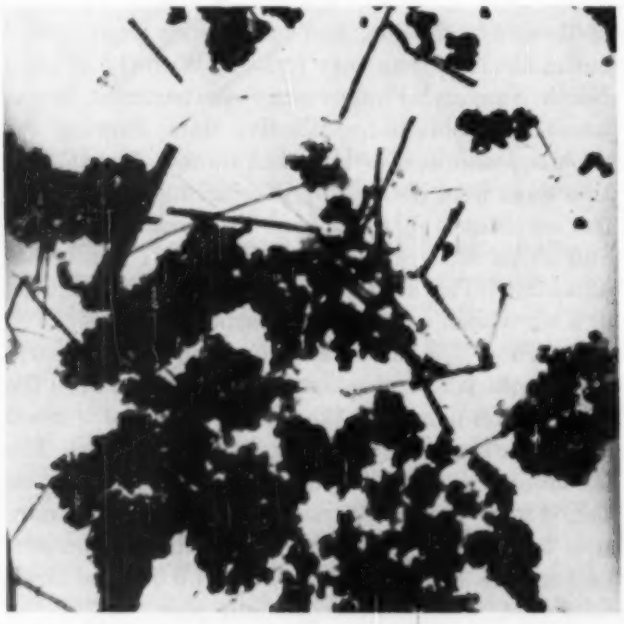

FIG. 3. Electron micrograph. Reaction product $SiO_2 + 3C = SiC + 2CO$. 1750°C for one-half hour. Size of equant particles approximate those of Fig. 2. Note layer or lamellar structure of rod-like skeletal crystals. 9,000×.

begins at a lower temperature, once started the silica-carbon reaction proceeds more rapidly. Each point plotted in Fig. 4 represents a single experimental run in the high frequency furnace held for one-half hour at the indicated temperature. In no case was there any indication of the formation of alpha SiC up to 2100°C.

Fig. 5 is based on Ruff's (8) method of following the progress of silicon carbide formation by the weight loss of the reaction mixture with increasing temperature. Curve A-1 of Fig. 4 and curve HF of Fig. 5 are similar in shape. While both curves originate from the same experiments, they are derived from different data. The first is based on chemical analysis,

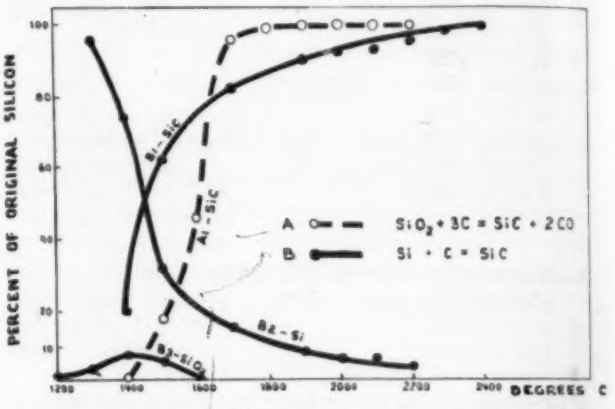

FIG. 4. Degree of silicon carbide formation as a function of temperature. All experiments held for one-half hour at temperature indicated by points. Curves were calculated on basis of silicon content of each component with silicon of original considered as 100. In this way the two different reactions could be directly compared.

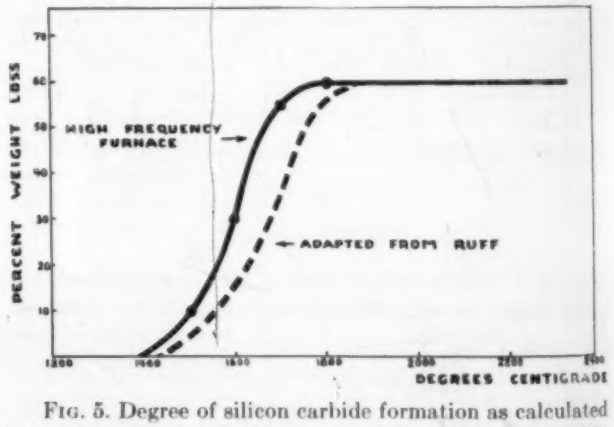

FIG. 5. Degree of silicon carbide formation as calculated from the weight loss in the reaction $SiO_2 + 3C = SiC + 2CO$. Compare these curves with Al-SiC of Fig. 4.

the second on the weight loss of silica-carbon mixes reacting to form silicon carbide. Ruff's curve and HF in Fig. 5 are very similar in form but slightly displaced. This is partly a time function, but also, as Ruff pointed out, the exact position of curves of this kind, even in his experiments, is a function of the kinds of carbon and silica used. The formation of silicon carbide from silica-carbon mixtures therefore always begins near 1500°C and is complete at or near 1800°C. Proudfoot (12), using comparable methods,

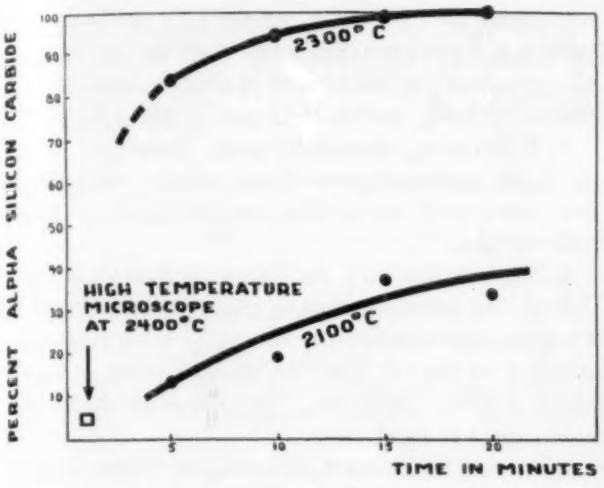

FIG. 6. Time-temperature relation of beta to alpha SiC based on x-ray diffraction analysis. Original SiC from reaction $SiO_2 + 3C = SiC + 2CO$.

FIG. 7. High temperature microscopy. The furnace at approximately 1750°C. Note fused quartz bubbles, and carbon being wet by molten silica.

FIG. 8. High temperature microscopy. Silica completely melted and reacting with inclosed carbon; note wisp of silicon vapor that has reached air. 1900°–2000°C.

has confirmed Ruff's statement that the CO pressure from this reaction reaches atmospheric pressure near 1500°C. If Fig. 1, based on calculations at atmospheric pressure, is again examined it is seen that $\Delta F^\circ = 0$ at 1500°C (curve 3). This also indicates that reduction of silica to silicon is the first step in

FIG. 9. High temperature microscopy. Primary SiC, apparently dendritic, as viewed at room temperature by transmitted light.

FIG. 10. Photomicrograph made by transmitted light of dendritic beta SiC obtained from reaction mix $SiO_2 + 3C = SiC + 2CO$, held at 2400°C in reaction chamber of high temperature microscope for one minute. 125×.

forming SiC. The final series, high frequency furnace experiments, consisted of four sets at 1800°, 2100°, 2200°, and 2300°C, respectively. The reaction mixture in each case was silica and carbon in the stoichiometrical proportion to form silicon carbide. At these temperatures, four runs, at 5, 10, 15, and 20 minutes

each at holding temperature, were made. Fig. 6 gives the data for the 2100° and 2300°C runs. Also, on Fig. 6 is a point obtained from analyzing the accumulated product of 60 high temperature runs in a microfurnace of a thermal microscope. The mean holding time at about 2400°C for these runs was one minute, and the percentage of beta SiC converted to alpha SiC was on the order of 5 per cent. When large enough beta SiC crystals are examined with the petrographic microscope under cross nicols, occasionally small included anisotropic areas may be observed, indicating the beginning of alpha SiC formation.

The Thermal Microscope Observation of SiC Formation

Fig. 7–9 are made from frames from motion pictures taken through a high temperature microscope described elsewhere (13). A mixture of powdered silica and carbon is placed in a one-eighth inch hole for a reaction chamber. Fig. 7 shows the silica fusing, and some of the silica forming bubbles which are picked up with slivers of carbon from the electrode. Fig. 8 shows the silica almost completely fused, and a wisp of silica formed by silicon vapor oxidizing to silica can be seen. Fig. 9 is a view taken cold of the primary silicon carbide formed by this type of experiment. Fig. 10 is a photomicrograph (250 diameter) of a part of the dendritic appearing crystalline mass shown in Fig. 9. These equant, anhedral particles are individual beta SiC that tend to aggregate on a skeletal crystal pattern. Although they have been at 2400°C for a minute, each particle is still essentially beta SiC.

Summary and Conclusions

1. Carbon reacts to form silicon carbide to a limited degree with the silicon of certain nickel-silicon or aluminum-silicon alloys at temperatures as low as 1000°C. Taylor and Laidlor (14) reported the formation of SiC from silicon and carbon at 1150°C, but here reaction was found only when some alloying agent reduced the liquifying point of silicon below 1400°C. Antipin and Ivanson (15) reported beta silicon carbide obtained from the electrolytic production of a silicon-aluminum alloy liquid at 1000°C in graphite crucibles.

2. With certain low melting alloys containing silicon and carbon, the reaction to form silicon carbide proceeds to a limited degree as low as 525°C, as in the example given of the composition zinc 53.3 per cent, aluminum 26.7 per cent, silicon 13.3 per cent, and carbon 6.7 per cent. Since the data on low melting alloys containing silicon are limited, experiments of this kind using known data are circumscribed.

3. When using chemically pure silicon and carbon in stoichiometrical proportions, silicon carbide was not formed until the melting point of silicon (1430°C) was reached.

4. The reaction to form silicon carbide from silica and carbon mixtures always begins near 1500°C. It is a two-step reaction, the first step being reduction of silica to silicon, and the second reaction being silicon carbide formation. The latter is almost instantaneous in most cases.

5. Primary SiC formed under all conditions studied is always beta SiC. Beta SiC is stable up to near 2100°C.

6. In none of the experiments did beta SiC show much crystal growth, maximum size crystals being less than 1.0 mm in diameter.

7. Beta SiC begins to transform monotropically to alpha SiC slowly at 2100°C. It changes to the alpha SiC form rapidly and completely at 2400°C.

Acknowledgment

The author wishes to acknowledge the assistance of G. L. Chapman and Gloria M. Faulring for their work in x-ray diffraction and electron microscopy, and of A. J. Orsey for his work in high temperature microscopy.

Any discussion of this paper will appear in a Discussion Section, to be published in the December 1952 issue of the Journal.

REFERENCES

1. N. W. Thibault, *Am. Mineral.*, **29**, 249, 327 (1944).
2. L. S. Ramsdell, *Am. Mineral.*, **32**, 64 (1947).
3. L. S. Ramsdell and J. A. Kohn, *Acta Crystal.*, **4**, Part 1, 75 (1951).
4. H. Ott, *Z. Krist.*, **63**, 1 (1926).
5. D. Lundquist, *Acta Chem. Scand.*, **2**, 177 (1948).
6. H. Baumhauer, *Z. Krist.*, **50**, 33 (1912).
7. H. Braekken, *Z. Krist.*, **75**, 572 (1930).
8. Otto Ruff, *Trans. Electrochem. Soc.*, **68**, 87 (1935).
9. C. G. Rose, *Brick & Clay Record*, **118**, 62 (1951).
10. H. L. Read, Refractories Div., Carborundum Co., Perth Amboy, N. J., Private Communication.
11. J. W. Gartland, *Trans. Electrochem. Soc.*, **38**, 121 (1945).
12. C. B. Proudfoot, Research & Development Division, Carborundum Co., Niagara Falls, N. Y., Personal communication.
13. H. N. Baumann, *Bull. Am. Ceram. Soc.*, **27**, 267 (1948).
14. A. Taylor and D. S. Laidlor, *Brit. J. Applied Phys.*, **1**, 174 (1950).
15. P. F. Antipin and L. I. Ivanson, *Doklady Akad. Nauk. S.S.S.R.*, **70**, 283 (1950).

The Synthesis, Fabrication, and Properties of Beryllium Carbide[1]

JOHN H. COOBS[2] AND WALTER J. KOSHUBA[3]

NEPA Division, Fairchild Engine and Airplane Corporation, Oak Ridge, Tennessee

ABSTRACT

The various methods that have been employed in synthesizing beryllium carbide are critically reviewed. Since beryllium carbide is an uncommon material, its known physical and chemical properties are described.

Because of its refractory nature and chemical instability in the presence of moisture, methods of fabricating beryllium carbide are definitely limited. Considerable success has, however, been achieved by hot-pressing techniques, and by means of cold-pressing followed by sintering under controlled conditions. Additions of graphite or of beryllium oxide to the carbide considerably facilitate fabrication.

The physical properties of fabricated beryllium carbide-base bodies are discussed in detail, and the effects of graphite or beryllium oxide additives on the properties of the bodies are disclosed.

INTRODUCTION

Beryllium carbide has been accorded very little attention until recently. Its existence has long been known as a scientific laboratory curiosity. In the beryllium industry, however, it occurs frequently in small amounts as one of the impurities which has plagued the beryllium melter over the years.

Liebmann (1) proposed for beryllium carbide the formula Be_4C_3, but the prior work of Lebeau (2), who reported that its composition is Be_2C, has since been verified by Stackelberg and Quatram (3) and by others. The meager data heretofore available on its physical and chemical properties have been reviewed and discussed by Geller (4).

Synthesis of Beryllium Carbide

The two general methods of preparing the carbide are based on the work of Lebeau (2), who heated mixtures of Be and charcoal and of BeO and charcoal in an electric furnace. Recent workers simply fired mixtures of BeO and charcoal in a graphite crucible, using induction heating. This product is black, and is high in free carbon and nitrogen. Chemical analyses have shown that the purity of the material prepared in such a manner would seldom exceed 80 per cent.

Fairly pure Be_2C was prepared by Stackelberg and Quatram (3), who pressed a mixture of BeO and charcoal into slugs and heated these to a temperature of 1930°C (3506°F) under a constant pressure of 30 psi in a vacuum furnace. By this means, a product 85 to 92 per cent pure may be obtained.

The preparation of small quantities of beryllium carbide has been accomplished at Battelle Memorial Institute by the reaction of molten beryllium metal with graphite. In this process, lump beryllium metal is melted and superheated in a graphite crucible. The molten metal reacts with the carbon of the crucible at 1700°–1800°C (3092°–3272°F) to form carbide, which gradually collects in the bottom of the melt as the reaction proceeds, until finally the whole mass solidifies. The product is recovered by leaching the beryllium metal with dilute HCl, and consists of well-formed crystals, usually light red and quite pure. The process is tedious and costly; only small quantities of beryllium carbide have been prepared by this means.

The synthesis of Be_2C in larger quantities has been accomplished at this laboratory by the reaction of beryllium oxide and carbon at high temperatures. In recent work, calcined beryllia and Acheson grade 2301 graphite have been used with good results. The reactants are mixed in stoichiometric proportions, with 1.5 per cent excess carbon to eliminate localized concentrations of BeO, and are then blended with 2 per cent by weight of paraffin binder. This mixture is then cold-pressed into compacts roughly 1.5 in. x 2 in. x 5 in., which are charged into a graphite crucible for subsequent firing.

The graphite crucible, 6 in. in diameter and 12 in. long, is loaded into an induction furnace composed of an induction coil, silica tube, and a graphite muffle tube insulated with thermatomic carbon. The crucible cover is provided with tubes for hydrogen flush-

[1] Manuscript received April 19, 1951. This paper prepared for delivery before the Washington Meeting, April 8 to 12, 1951.

[2] Present address: Oak Ridge National Laboratory, Carbide and Carbon Chemicals Division, Union Carbide and Carbon Corporation, P. O. Box P, Oak Ridge, Tennessee.

[3] Present address: General Electric Company, AGTD, ANP Project, P. O. Box 125, Oak Ridge, Tennessee.

ing and with a blind-end sight tube. The whole assembly is covered with an exhaust duct. Since Be_2C readily absorbs nitrogen at high temperatures, all charges must be heated, fired, and cooled under an atmosphere of purified hydrogen.

The charge is fired for 2½ to 4 hours at a temperature of 2000°–2300°C (3632°–4172°F); the optimum temperature is about 2230°C (4046°F). Recent work has shown that good quality material may be prepared by firing in the range 1950°–2100°C (3542°–3812°F) for a period of about 8 hours.

The product from these runs is composed of a loosely bonded mass of small, clear crystals, quite friable, and varying in color from amber through light red to dark gray. This mass is broken up and the product graded according to color and texture. In all cases, there is some unreacted material remaining which is not recycled. The yield of usable product averages around 2 pounds or 80 per cent of the theoretical amount.

Properties of Beryllium Carbide

Since Be_2C in contact with moist air at room temperature is progressively hydrolyzed to form $Be(OH)_2$, all raw material and fabricated specimens must be stored in sealed desiccated containers. This raw material is typically 90–96 per cent pure Be_2C, whose major impurities are beryllium nitride, free beryllium oxide, and free carbon, each occurring to the extent of roughly 1–3 per cent.

The analytical methods for BeO and free C in Be_2C are quite tedious and require special equipment. BeO is determined as the residue from bromination, and graphitic carbon is collected as the residue from decomposition of the Be_2C in strong acids. However, the standard Kjeldahl method for nitrogen gives reproducible results with this material.

Be_2C crystallizes in the cubic system; it is octahedral in habit and has the antifluorite crystal structure. The lattice parameter is 4.34 Å, giving a theoretical density of 2.44 g/cm³. The octahedral crystals are very sharply developed, with brilliant faces. They have a refractive index of 2.75. The Knoop hardness of Be_2C is 2690; this is harder than silicon carbide and approaches the hardness of boron carbide.

Fabrication of Beryllium Carbide

Due to the nature of the material, the only practicable methods available for the fabrication of beryllium carbide bodies involve dry ceramic techniques and powder metallurgical procedures, requiring either cold-pressing and sintering, or hot-pressing. Standard ceramic methods of fabrication, such as slip casting and extrusion, have not been successful to date.

Cold Pressing

Early attempts at fabrication by sintering were conducted by grinding the material in a porcelain mill, incorporating 7.5 per cent paraffin binder, cold-pressing at pressures up to 36,000 psi, and sintering at 1870°C (3398°F) in an argon atmosphere. The resulting specimens in general were coarse grained and had relatively poor physical properties, with porosities ranging from 30–50 per cent and an average compressive strength of 13,000 psi.

Attempts were then made to develop a bond by the reaction of pitch and beryllium metal additions. Various proportions of pitch and beryllium metal were added to the ground Be_2C by hot-mixing at 150°C (302°F). The mixtures were pressed into compacts, heated slowly to 900°C (1652°F), and finally sintered at 1870°C (3398°F) in argon. Optimum proportions for the bond seemed to be 15 per cent pitch and 7 per cent Be metal additions to the Be_2C, but again results were not encouraging.

In another experiment, compacts pressed from powder ground to −325 mesh in a BeO-lined mill with BeO balls were packed into a sleeve made of BeO powder; this was placed in a graphite crucible and fired at 2230°C (4046°F) for 40 minutes in argon. These specimens all had laminar cracks from the cold-pressing operation. In general, those compacts prepared from material of finer particle size had somewhat higher bulk densities, but also had more voids and were more fragile. Modulus of rupture values for these specimens were in the range of 5000–8000 psi.

During this early work, it was found that Be_2C undergoes thermal decomposition at high temperatures where recrystallization or grain growth would normally be expected to occur. This decomposition occurs rapidly above 2300°C (4172°F), yielding beryllium vapor and a residue of graphite. It has been determined that the vapor pressure curve of beryllium in equilibrium with Be_2C is nearly coincident with that of beryllium vapor in equilibrium with molten beryllium (5). Thus, it became obvious that bonding agents in the form of metals or oxides must be incorporated or that special techniques must be developed, in order that the material may be fired to maturity without decomposition.

Cold-pressing and sintering techniques have been developed by Battelle Memorial Institute for preparing Be_2C bodies. In this process, the Be_2C is hydrostatically pressed at 50,000–75,000 psi into rods roughly 3/4 in. diameter x 10 in. long, and are sintered for 30 minutes at 2250°–2300°C (4082°–4172°F) in a protective atmosphere. This results in a fairly dense, strong body.

Recent work with additions of 10 per cent of metals such as Fe, Al, and Si has indicated some promise. The mixtures were fabricated by the Bat-

telle procedure except for sintering at slightly lower temperatures. Of the metals tried, Fe and Si are the most promising from the standpoint of bonding additions.

The metal addition seems to act as a flux, readily forming an intergranular bond. X-ray data on lattice constant shifts show no appreciable solubility of the metals in Be_2C, but afford evidence of some solubility of Be and C in iron, for instance. No physical properties are available on these compositions.

Hot-Pressing

Fabrication of Be_2C bodies is readily facilitated by the hot-pressing techniques developed in the NEPA laboratories. In this process, it is necessary that the Be_2C be quite fine, with a particle size distribution of roughly 10–40 microns. Consolidation is greatly facilitated by the addition of a few per cent of bonding agents, such as graphite or beryllium oxide.

The raw material as received is first ground for 48 hours in a 4-quart rubber-lined mill using steel balls; this process introduces roughly 1.5–2 per cent iron. Batches which are to contain graphite as bonding agent are then mixed for an additional 6 hours in the same mill with the requisite amount of Acheson grade 2301 graphite powder.

In the preparation of some shapes, it is desirable that the charge material have a high loading density in the dies; for these purposes, the ground and mixed material is pre-pressed cold at 60,000 psi, and is reground to pass 20 mesh.

Since all work on the hot-pressing of Be_2C is performed at temperatures ranging from 1900°–2200°C (3452°–3992°F), the only material suitable for dies is graphite. As compared with most die materials, graphite is relatively weak and soft, but it has a distinct advantage in that its strength is not greatly reduced up to about 2300°C (4172°F). In general, it is desirable to use fairly high pressures in order to promote consolidation, but in most cases pressure must be limited to 2000 psi in order that the die block be of reasonable size. Dies currently in use are designed for a maximum pressure of 2000–2500 psi on the punches at 2000°C (3992°F). These dies have a useful life of 6–10 runs. All dies are designed for use with protective atmospheres. The dimensions of the most useful designs are presented in Table I.

A typical furnace assembly is illustrated in Fig. 1. It consists of an induction coil, refractory liner, and a graphite muffle tube insulated with thermatomic carbon. The die is placed inside the graphite muffle. Pressure is applied to the die assembly by means of carbon bricks, or porous carbon punches machined from National Carbon grade 60 Carbocel. This furnace is used in conjunction with a 40-kw Ajax mercury-arc, high frequency generator, and a 75-ton frame press; the latter is equipped with a hydraulic pump for maintaining constant pressure on the punches at any pre-set value.

Temperature is measured by means of an optical pyrometer, sighting through a prism into the sight hole, which is drilled to within 1 in. of the specimen. The graphite sight tube is kept clear of fumes by a constant downward stream of hydrogen.

The dies are prepared for loading by coating the die walls and the faces of the punches with graphite by means of a die wash. This die wash is prepared as a suspension of 1 gram of Dixon 200–10 micronized graphite in 7 ml of CCl_4; it is useful in preventing the compact from reacting with and sticking to the die walls, with resultant excessive die wear and breakage of a high proportion of compacts.

After charging with the powder to be pressed, the die assembly is cold-pressed at 1000 psi and loaded into the hot-press furnace. The furnace is purged with hydrogen for about an hour, and then is heated. Fig. 2 illustrates the time-temperature-pressure relationships during a typical heating cycle. The pres-

TABLE I. *Dimensions of some graphite dies for hot pressing beryllium carbide*

Outside diameter	Length	Inside dimension
in.	in.	in.
6	6	2 (diameter)
8	6	3 x 3
9	6	1½ x 5
10	10	4½ (diameter)

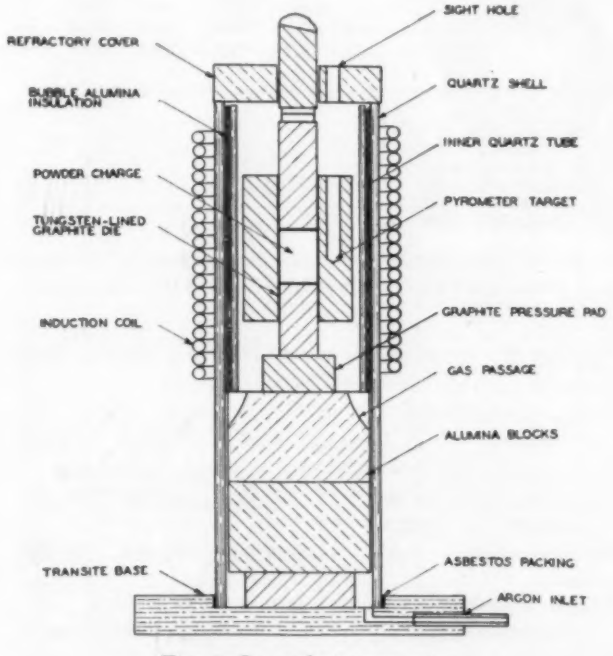

FIG. 1. Large hot-press setup

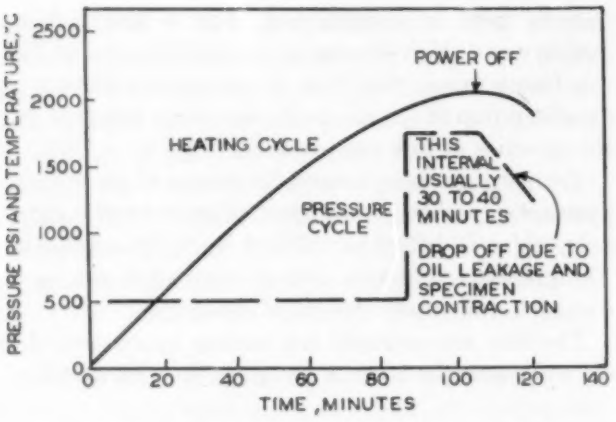

FIG. 2. Temperature pressure relationships for hot-press pressing.

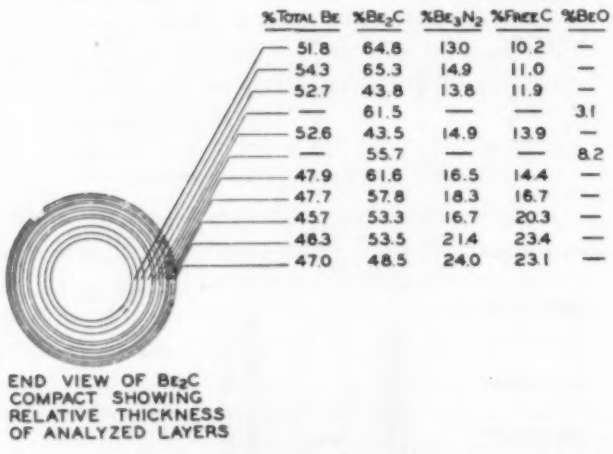

FIG. 3. Analysis of layers machined from a Be_2C compact hot-pressed at 2100°C, 3500 psi, and in a CO–N_2 atmosphere.

TABLE II. *Properties of hot-pressed and sintered* Be_2C-*base bodies*

Property	Units	Be_2C	90% Be_2C–10% C	Sintered Be_2C
Compressive strength	psi	105,000	102,000	71,000
Modulus of rupture	psi	13–14,000	11,900	11,000
Elastic modulus (compression)	psi	$45.6 \cdot 10^6$	$29.6 \cdot 10^6$	—
Elastic modulus (flexure)	psi	$50.5 \cdot 10^6$	$46.1 \cdot 10^6$	—
Poisson's ratio		0.10	0.11	—
Thermal conductivity	BTU/hr/ft²/°F/ft	13.5 (300°F)	18.0 (300°F)	—
Coefficient of expansion	in./in./°F	$7.47 \cdot 10^{-6}$	$7.4 \cdot 10^{-6}$	—
Electrical resistivity	ohm-cm	1.1	0.14	—
Theoretical density	g/cm³	2.44	2.42	2.44
Apparent density	g/cm³	2.26	2.37	2.1
Porosity	%	6–8	2–3	15

sure is maintained at 500 psi until a temperature of 1950°C (3542°F) is reached, whereupon the pressure is raised to 2000 psi and held for 30 minutes while a maximum temperature of 2030°–2050°C (3686°–3722°F) is attained. This maximum temperature is quite critical. Since Be_2C does not melt, and does not exhibit appreciable plasticity, one must utilize the highest temperature practicable in order to achieve some degree of grain growth. However, if the critical range is exceeded by even 50°C (90°F) the material begins to decompose, and attacks the die walls severely.

Just as with the synthesis of raw material, all hot-pressing operations must be carried out in a hydrogen atmosphere. The hydrogen is purified by passing it through a palladium catalyst, thence through magnesium perchlorate, and finally through a liquid nitrogen cold trap. It is then admitted to the furnace from the bottom and directed upward through the punch to within 1 in. of the specimen.

Fig. 3 shows the results from chemical analyses of concentric rings machined from a specimen that was hot-pressed without a protective hydrogen atmosphere. As much as 12 per cent nitrogen has been absorbed by the Be_2C near the surface of the body, while even near the center of the body more than half that amount is reported. Consequently, if reproducible, homogeneous bodies are to be obtained, it is quite evident that some protective atmosphere must be utilized. Helium and argon have been tested for this purpose, but hydrogen seems to the most efficient.

As prepared in this manner, the Be_2C base bodies are quite strong and relatively hard. Machining of test specimens is accomplished by utilizing Felker Dimet cut-off wheels and Norton bonded diamond grinding wheels, on machines equipped with high-velocity exhaust systems. Socony-Vacuum "Vacmul B-1" is employed as lubricant and coolant for all machining operations, and may be removed from finished specimens by refluxing dry ether over the bodies in a Soxhlet extractor.

Properties of Fabricated Beryllium Carbide Bodies

The important physical properties of hot-pressed Be_2C base bodies, as well as the limited data available on sintered specimens, are presented in Table II for comparison. Physical property data on the hydrostatically pressed and sintered specimens are incomplete, due to the wide variations in properties inherent in these bodies. Also, no data on sintered 90 per cent Be_2C-10 per cent C specimens are available for comparison with hot-pressed bodies of this composition, since bodies containing graphite are not inherently amenable to fabrication by sintering.

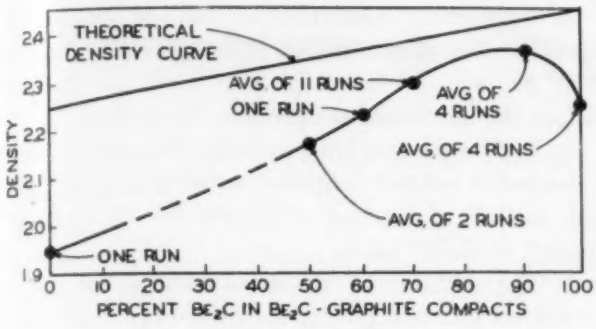

FIG. 4. Plot of density vs. composition for hot-pressed Be_2C-graphite compacts.

in this proportion the graphite is most efficient in promoting consolidation. In higher concentrations, the graphite adversely affects the density, and the porosity increases.

In Table III, the properties of hot-pressed Be_2C-BeO compositions are presented for comparison.

In general, the values for mechanical properties increase as the proportion of BeO is increased. This is especially true of compressive strength and modulus of rupture, which may explain to some extent why the modulus of rupture values on the sintered Be_2C specimens, which contain appreciable quantities of BeO, compare favorably with values on low-porosity, hot-pressed Be_2C bodies.

Since Be_2C is quite refractory, its mechanical

TABLE III. *Properties of hot-pressed* Be_2C–BeO *compositions*

Property	Units Be_2C		80% Be_2C–20% BeO	60% Be_2C–40% BeO	BeO
Compressive strength	psi	105,000	—	128,000	186,000
Modulus of rupture	psi	13–14,000	14,800	22,600	18,900
Elastic modulus (compression)	psi	$45.6 \cdot 10^6$		$44.7 \cdot 10^6$	$54.6 \cdot 10^6$
Elastic modulus (flexure)	psi	$40.5 \cdot 10^6$	$16.3 \cdot 10^6$	—	$45.2 \cdot 10^6$
Poisson's ratio		0.10	—	0.19	0.18
Electrical resistivity	ohm-cm	1.1	4.13	10.9	$7 \cdot 10^9$
Theoretical density	g/cm³	2.44	2.54	2.65	3.03
Apparent density	g/cm³	2.26	2.4	2.60	2.93
Porosity	%	6–8%	4–5%	2–3%	3%

TABLE IV. *Variation of elastic modulus with temperature*

	Elastic modulus (compression) psi · 10^6			
	Room temperature	1000°F	1500°F	2000°F
Be_2C	45.6	45.6	35	30
90%Be_2C—10%C	29.6	29.6	25	—

The values for the modulus of rupture of the three compositions compare favorably, and the compressive strengths are not widely different, indicating little or no correlation between porosity and ultimate strength.

The mechanical properties of the two hot-pressed compositions are seen to be roughly parallel. The graphite addition does not appreciably affect the thermal expansion, since it is assimilated in the pores and grain boundaries, and forms only a small part of the total volume. It increases the thermal conductivity appreciably, and lowers the specific resistance by an order of magnitude, as would be expected. The most significant effect of the graphite, however, is the higher apparent density and very low porosity obtained because of the reduction of intergranular friction during consolidation. This effect is illustrated in Fig. 4, showing the curve of densities obtained on various compositions of Be_2C plus graphite as compared to the theoretical density curve. The peak in the curve near the 90 per cent Be_2C-10 per cent C composition shows that

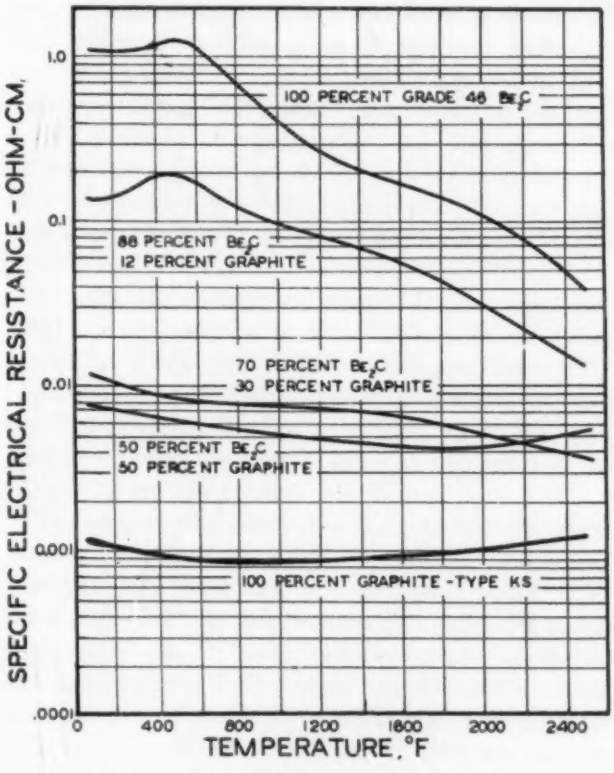

FIG. 5. Electrical resistivity vs. temperature for Be_2C-graphite bodies of various compositions.

properties are not drastically affected by temperature.

In Table IV, the effect of temperature on the elastic modulus of Be_2C and of 90 per cent Be_2C-10 per cent C is illustrated. At 1500°F the moduli have been lowered by 23 and 18 per cent, respectively.

In Fig. 5, the curve of electrical resistivity vs. temperature shows normal decline in specific resistance with increasing temperature for those compositions high in Be_2C. However, the 50 per cent Be_2C-50 per cent C composition, in which the graphite phase is continuous, exhibits behavior analogous to that of type KS graphite.

Conclusions

On the basis of the results obtained in this work, several conclusions may be drawn:

1. Be_2C bodies may be fabricated by hydrostatic pressing, and by sintering the finely ground material. However, these bodies are likely to show considerable variation in mechanical properties, porosity, and purity.

2. Commercial grade Be_2C (90–96 per cent pure) may be fabricated into useful shapes by hot-pressing the finely ground material in graphite dies.

3. Satisfactory conditions for the hot-pressing of Be_2C are temperatures of 2030°–2050°C (3686°–3722°F), and pressures of 2000–2500 psi applied before the maximum temperature is reached.

4. Be_2C specimens hot-pressed in this manner may be expected to have compressive strengths of 100,000 psi, moduli of rupture of 13,000 psi, and elastic moduli of $45 \cdot 10^6$ psi.

5. The addition of small percentages of finely powdered graphite greatly facilitates the consolidation of Be_2C bodies by hot-pressing; with the exception of lower porosity and electrical resistivity, the resulting bodies will have roughly the same properties as nominally pure Be_2C.

Any discussion of this paper will appear in a Discussion Section, to be published in the December 1952 issue of the Journal.

References

1. Liebmann, German Pat. 101,326 (1898).
2. P. Lebeau, *Compt. rend.*, **121**, 496 (1895).
3. M. v. Stackelberg and F. Quatram, *Z. physik. Chem.*, **B27**, 50 (1934).
4. R. F. Geller, *Nucleonics*, **7**, No. 4, 3 (1950).
5. J. Kielland and L. Tronstadt, *Kgl. Norske Videnskab. Selskabs., Forh.*, **8**, 147 (1935) (published in 1936).

A Spectrophotometric Study of the Oxidation of Tantalum[1]

J. T. Waber, G. E. Sturdy, E. M. Wise[2], and C. R. Tipton, Jr.*

Los Alamos Scientific Laboratory, Los Alamos, New Mexico

ABSTRACT

Collateral spectrophotometric and gravimetric studies of the air oxidation of tantalum have been conducted over the range of 220° to 350°C. Good reproducibility of data was observed. This metal obeys a logarithmic law up to 320°C and a parabolic law above. Arrhenius plots of the logarithmic rate law data give temperature dependences of 12.57 kcal/mole on the basis of the microgravimetric method and 12.0 kcal/mole from the spectrophotometric method. The Arrhenius plot of initial parabolic rate law data gives 27.2 kcal/mole in good agreement with a previous value obtained by Gulbransen and Andrew. The two methods have been used to estimate the ratio of true to apparent surface area to be 10.

Introduction

The primary objective of this work was a comparison of corrosion of tantalum as determined by spectrophotometric methods and by weight change as measured by a microbalance.

Although the development and application of spectrophotometric methods to the corrosion of metals is not unique, its general use has not been realized because of the unavailability of spectrophotometers. Previous unpublished data obtained by one of the authors indicated that the recording spectrophotometer could be employed to analyze the interference colors which occur during oxidation.

At the outset of this investigation only two preliminary studies were available which related to the oxidation resistance of tantalum: limited quantitative data in the Corrosion Handbook (1) and a tentative curve in the report of McAdams and Geil (2). During the preparation of this report, Gulbransen and Andrew (3) published a more detailed study over the range of 250° to 450°C. The following research was initiated in order to study the low temperature oxidation behavior of this metal more adequately. Further, there was not available any extensive study of the oxidation of a common metal by the spectrophotometric method where collateral studies had also been made with a microbalance.

Preliminary analysis of Balke's data (1) led to the conclusion that the oxidation reaction was controlled by the diffusion of ions through the coherent oxide layer. A parabolic law usually described such diffusion control although occasionally a logarithmic growth law is encountered. It was apparent that the data past five hundred hours were not in agreement with a parabolic law. Subsequent confirmation of the inadequacy of the parabolic rate equation was obtained with the microgravimetric data.

Plotting the logarithm of the weight gain rate, $\Delta W/\Delta T$, against the reciprocal of average temperature gives a line of slope 5.00, from which an energy of activation of 22.9 kcal was calculated.

The work of Gulbransen and Andrew (3) indicates that the parabolic growth law satisfies the weight-gain data for the 120-minute period employed. The best information of this research, however, indicates that the oxidation follows a logarithmic growth law over considerable periods of time, but indicates that early rates can be adequately treated as parabolic growth laws. These parabolic rate data have been used to obtain the energy of activation as have the rate data obtained from the longer term logarithmic growth law.

The spectrophotometric studies involve measurement of the reflectance of a surface as oxidation proceeds. While this technique has not been fully exploited, the preliminary investigations are interesting. Using the method of reflectance there is a possibility of measuring oxide films in the order of 10 Å with an accuracy much better than 5 Å.

The simple color method of gauging film thickness has been used several times in the past. It is assumed that the color produced by a film on a metal is determined solely by the wavelength suffering maximum extinction. It then becomes possible to obtain the approximate thickness of any film by dividing the thickness of an air film needed to give the equivalent colors (i.e., Newton Ring Colors) by the refractive index of the film substance.

Bannister and Evans (4) studied the attack of iodine on silver metal and employed, in addition to the color thickness method, gravimetric, electrometric, and nephelometric[3] determinations. The

[1] Manuscript received July 9, 1951. This paper prepared for delivery before the Detroit Meeting, October 9 to 12, 1951. Work done under the auspices of the Atomic Energy Commission.

[2] Present address: University of Kansas, Lawrence, Kansas.

* Present address: Battelle Memorial Institute, Columbus, Ohio.

[3] Chemical determination of iodine in solution after reduction of the iodide film.

latter three gave good agreement among themselves, but the color method gave discordant results. It is now known that discrepancy occurs because there is a phase shift in the wavelength of light upon reflection from a metallic surface. This shift is equivalent to about 150 Å of oxide.

The most careful analysis of the spectrophotometric methods to date has been made by Constable at Cambridge. His initial studies (5) were on the colors given by the oxidation of metallic copper. Subsequently, he studied the growth of oxide films on iron, nickel, and copper (6). Due to the high optical dispersion of nickel oxide and ferric oxide, it was possible to obtain second order interference colors before the first had disappeared.

The only other significant optical method for measuring film thicknesses depends upon polarization (7–9). This method requires a number of measurements for each determination of oxide thickness and considerable calculation to obtain the necessary information for the growth law. In contrast, the spectrophotometric method, although only applicable to large oxide thicknesses, requires a matter of minutes and the data are easier to manipulate for calculation.

Experimental Procedure

High purity tantalum was rolled to 0.127-cm thickness. Small squares about 3.17 cm on an edge were measured to obtain the apparent area and then were carefully polished with "used" emery paper to a 4/0 finish. The specimens were cleaned in alcohol, rinsed in ether, and dried in an air blast; if staining occurred the specimens were repolished. The individual specimens were held in porcelain holders in the furnaces and all manipulations were made with bone forceps. Profilometer checks gave 14 microinches per inch as the smoothness. No detectable loss of oxide resulted from handling during the weighing operation or from the positioning of the sample in the spectrophotometer.

The furnaces were maintained at temperatures by a specially designed multipoint controller activated by a Selectoray control unit. The temperature of each individual furnace was checked by means of independent and calibrated thermocouples. Temperature patterns were not investigated within the individual furnaces, but it was thought that the variation was adequately low.

The spectrophotometer was of the G.-E. Hardy type, wherein the specimen is illuminated by light polarized in the plane of incidence. As inadequate alignment of the polishing direction causes scatter about the true curve representing the data, the polishing direction should be parallel to the plane of incidence for best results.

The specimens were heated at each of four temperatures for about 24 hours and cooled to room temperature. When cool, a spectrophotometer run was made and the weight of each specimen was taken. The specimen was then replaced in the porcelain holder and returned to the furnace for another cycle. Only the actual time in the furnace was used in calculating the elapsed time at temperature. When data were taken more frequently, a small correction for heating time was subtracted in the calculation of the time at temperature.

The microbalance used was an Ainsworth Type FDJ operating on the principle of an optical lever. The platform for the balance case was suspended from a vibration-free beam and damped in a modified Julius suspension. Special precautions were taken to eliminate electrostatic effects by placing a millicurie gamma-ray source and a humidifier within the balance case. A set of Class M weights, calibrated to higher accuracy by substitution weighing, was employed in the routine weighing. No special care, such as air conditioning, was taken to avoid thermal convection currents in the balance case or to avoid humidity variations that would affect the absolute weight of the calibrated weights. Even in the absence of these precautions the reproducibility was better than 0.75 $\mu g/cm^2$ on a 5-gram sample.

Spectrophotometric Results

The spectrophotometer measured the reflectance of the oxidized samples. When the oxide has grown to a certain thickness there is destructive interference between the light reflected from the metal-oxide interface and that from oxide-gas interface. Hence a minimum in the reflectance occurs for the wavelength.

The wavelength of a minimum can be read from the curve drawn by the machine to 50 or 100 Å which, however, is equivalent to only 5 or 10 Å error in oxide thickness. This can be reduced by using the direct reading wavelength dial. The minimum can be detected by watching the percentage reflection dial as the minimum is passed and marking the wavelength on the graph with the stylus. The wavelength scale was frequently checked against a didynium glass standard.

Since the wavelength minimum of the reflectance curve is directly proportional to the thickness of the oxide film, it is proper to plot these minima as a function of time. At the two higher temperatures, two curves corresponding to first and second order interference colors are included on each plot. As is typical of the progression of interference colors, there is a small hiatus (in time) when there is no minimum in the visible range, but a second order interference occurs in the near ultraviolet.

The spectrophotometric data gave the best fit

when plotted against the logarithm of the elapsed time. The usual expression for a logarithmic growth law is

$$y = K_1 \ln (t + 1) \qquad \text{(I)}$$

wherein y is the thickness of oxide, t is the time in hours, and K_1 is the logarithmic rate constant.

A typical curve for specimens exposed to 350°C is given in Fig. 1. A slight modification is necessary to relate thickness to the wavelength of the reflectance minima since there is a phase shift upon reflectance at an interface. Three such interfaces occur when a ray of light transverses an oxide layer on a metal. It is conventional to express the resultant phase shift in units of equivalent oxide thickness rather than in the more accurate angular measure.

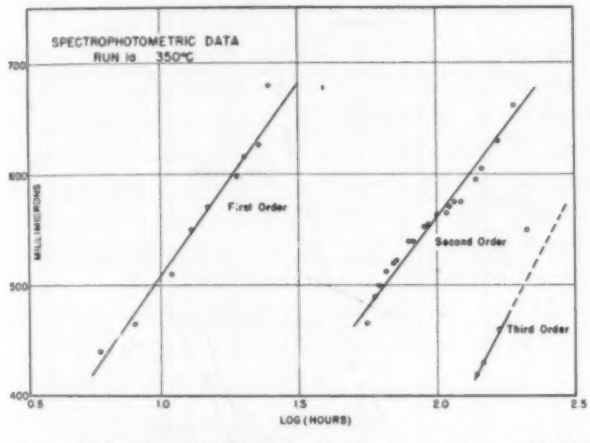

FIG. 1. Spectrophotometric data, Run 1A at 550°C. Minima plotted against the logarithm of time.

When the oxide is y Å thick it appears that the oxide is $y + \delta$ units thick as far as destructive interference is concerned. A minimum in the spectrometer trace occurs at λ Å when the oxide is y units thick. The relation connecting these is due to Evans (10) and is

$$y + \delta = \frac{(2n + 1)\lambda}{4\eta} \qquad \text{(II)}$$

where n is the order of the interference color and η is the refractive index of the oxide at a wavelength λ Å. The wavelength can be expressed by

$$\lambda - \Delta = \frac{(4\eta K_1)}{2n + 1} \ln(t + 1) \qquad \text{(III)}$$

where $\Delta = 4\eta\delta/(2n + 1)$.

Therefore it is appropriate to plot λ against the logarithm of the elapsed time since t was large compared to one. However, when t is not large compared to unity, a decreasing deviation from the straight line occurs. For this reason an accurate determination of the quantity δ is difficult.

Microgravimetric Results

The weight-gain data, for the range 230° to 350°C, can be condensed in plots similar to Fig. 2. The reproducibility of the microbalance weighings and of the surface preparation is characterized by good agreement between duplicate specimens oxidized at 350°C. A summary of the total weight increases are given in Table I. Duplicate runs 1A and 2A agree to one per cent. The logarithmic growth law suggested in previous sections is confirmed by the data obtained with the microbalance. The period of exposure to the temperature was long enough to justify this conclusion.

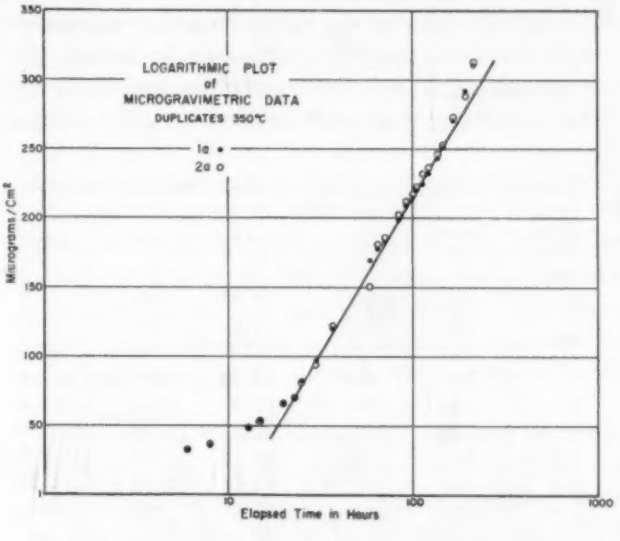

FIG. 2. Logarithmic plot of weight gain versus elapsed time. Specimens 1A and 2A at 350°C.

Calculation of Oxide Thicknesses

To compare the results obtained by both methods it is desirable to convert them to the common basis of oxide thickness. The spectrophotometric data can be converted to apparent thickness T_0 or $y + \delta$ by equation (II) if the oxide refractive index is known for each wavelength. A geometric mean refractive index of the orthorhombic tantalum pentoxide and its optical dispersion can be represented by the Cauchy formula, to a sufficient degree of accuracy for interpolation, as

$$n(\lambda) = 2.033 + 8.74 \cdot 10^6/\lambda^2. \qquad \text{(IV)}$$

The coefficients are based on the geometric mean of the three indexes and the measured dispersion coefficient obtained for the index in the gamma direction, the data for which were obtained here.

The gravimetric thickness in Å can be calculated from

$$T_w = 10^8 WG/\rho \qquad \text{(V)}$$

where W is the weight increase in g/cm², G is the gravimetric constant for calculating oxide from oxygen, and ρ is the density. A handbook value of the x-ray density, namely, 8.735 g/cm³, was used.

Comparison of Results Obtained by the Two Methods

Typical data are plotted in Fig. 3 for runs 1A and 2A. Straight lines are obtained for both the first and second order interference colors.

The slope of the first order line is greater than one and this is interpreted as a measure of the surface area ratio. The lines intersect the abscissa as is expected if a positive phase shift, δ, occurred during surface reflection of the light. There is an apparent oxide thickness despite a zero gain in weight. The slope calculated for the first order line from this plot is 10.0 and that obtained from a similar analysis

TABLE I. *Summary of the oxidation data for tantalum*

Sample No.	Temperature °C	Hours	Area cm²	Wt gain (μg)	μg/cm²
1	220	913	14.38	305.7	21.26
2	220	913	13.18	266.9	20.25
3	250	1434	13.44	897.0	66.74
4	320	913	11.52	2624.7	227.84
5	350	1237.5	11.80	6751.1	572.30
6	350	1237.5	12.57	6335.0	503.98
1-A	350	212.5	14.38	4466.6	310.61
2-A	350	212.5	13.18	4140.5	314.15
6-A	320	232	12.57	140.2	11.15

of run No. 3 is 9.75. A simple computation shows that the ratio of true to apparent surface area for three samples is

$$\beta = \frac{\text{True area}}{\text{Apparent}} = 9.92 \pm 0.07 \qquad \text{(VI)}$$

which is precise average deviation to better than seven tenths of a per cent. The probable error is 0.08 units.

The surface area ratio is offered as the explanation of the slope, in this comparison plot. This interpretation, which leads to an apparently high value for the ratio, is subject to the criticism of Willkins (11) who pointed out that surface cracks, etc., having dimensions of 10^{-5} cm, cannot be detected by optical methods. He also demonstrated that some metal was trapped in the oxide films when copper is oxidized. Thus, he felt that the ratio of true to apparent area should be low when determined from spectrophotometric data.

An alternate explanation of the large ratio is that part of the oxide dissolves in the metal and the film is thinner than that indicated by the weight increase. Such reaction would probably be diffusion controlled and so temperature dependent. Runs at 250° and 350°C gave almost identical values of β so that this second explanation seems to be unlikely.

Kinetics of the Reaction[4]

Theoretical studies have likened a diffusion-controlled scaling reaction to a galvanic cell with a gas electrode. In this model, the coherent corrosion products act as a polar solvent and dissolved ions provide necessary conduction. Surface adsorbed gas is consumed as at a gas electrode. Cations form at the metal interface. The driving force for ions is the voltage which is equivalent to the free energy change

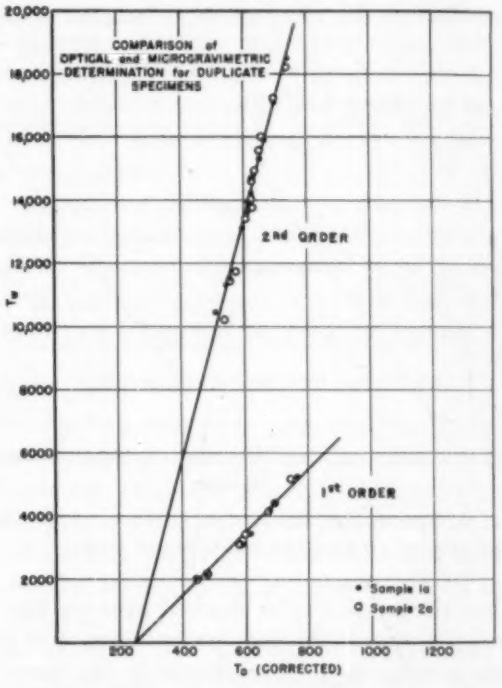

FIG. 3. A comparison of optical T_0 and microgravimetric T_w determinations of thickness for duplicate specimens.

accompanying the corrosion reaction. It would seem that because of the law of multiple proportions the concentration gradients would be steep and discontinuous. This is equivalent to strong polarization of the galvanic cell. However, either lattice vacancies or interstitial ions may dissolve in the oxide and either can diffuse. It is these factors which bring about departure from this law. Once diffusion can occur under an imposed driving force a smooth concentration gradient can be stabilized.

When the concentration gradient is just a simple inverse function of the film thickness, i.e., $\Delta c/y$, the flux of ions decreases slowly with time. Mathemati-

[4] Additional material supporting the assumptions in this section has been presented by Waber, *et al.*, in AEC document AECU 1355, Technical Information Service, Oak Ridge, Tennessee.

cally, the total current J, passing the interface in gram ions per second, is

$$\frac{D\Delta c\beta A}{y} = J \qquad \text{(VII)}$$

where D is the ionic diffusivity in gram ions cm²/sec, βA the true surface area, Δc the concentration difference of lattice vacancies or interstitial ions at the inner and outer interfaces of the oxide in numbers of ions per cm³, and y the thickness.

It may be expected that the corrosion rate is governed by rate of arrival of cations at the outer surface and by the concentration of oxygen atoms adsorbed there. Hence in terms of units of reaction r the rate is

$$\frac{dr}{dt} = kJP^{\nu} \qquad \text{(VIII)}$$

where k is a simple number (1/2) adjusting gram atoms to the units of reaction, P is partial pressure of the oxygen, and ν is an experimental constant. Here the concentration of adsorbed atoms is given by Freudlich's adsorption isotherm which is, in general, valid at high partial pressures. The expected magnitude of ν is less than one. Replacing current per unit area from (8) by the equivalent expression in which the thickness y is the explicit variable by multiplying by the molar volume of the products per mole of cations gives

$$\frac{dy}{dt} = \frac{D\Delta c\Omega P^{\nu}}{y} \qquad \text{(VIII}a\text{)}$$

where the factor k has been dropped because of the definition of molar volume of the corrosion product, Ω, and ν. Alternately, from the integrated form, and with thickness replaced by weight gain per unit area, W,

$$W^2 = BP^{\nu}t + \text{constant} \qquad \text{(IX)}$$

where B is a specific rate constant independent of pressure. The constant of integration is usually zero, as the weight increase at zero time is conventionally chosen to be zero. A further condition for integration is that the reaction does not cause a significant change in the pressure, i.e., P is not function of time.

By direct chemical means Wagner and his coworkers (12) were able to show that departure from ideal stoichiometric composition of materials, such as cuprous oxide, showed a low pressure dependence; namely, a small fractional power of the ambient pressure. It was then clear that the concentration of lattice vacancies or of interstitial ions was related in a similar fashion to the imposed gas pressure.

In Wagner's theory of metal-oxygen reactions, there is an intimate connection between the electrical conductivity of the semiconducting oxide layers and the rate of oxidation reaction. Both are related to the diffusion of ions through the oxide. It has been found that the dependence of conductivity on the oxygen pressure exerted over the oxide can be expressed as

$$\sigma = \sigma_0 P^{\mu} \qquad \text{(X)}$$

where σ is the conductivity observed at pressure P, and σ_0 is that at one atmosphere. The value of μ may be positive or negative, depending on whether the oxide is a cationic or anionic defect type conductor, respectively. In magnitude, μ lies in the range of 1/7 to 1/3.

When an alloy containing an intentional impurity is oxidized, the effect on the corrosion rate is in agreement with the effect predicted from experience on the electrical conductivity of ionic compounds and the effect of impurities on it. It is difficult to see how minor additions can affect the concentration of adsorbed gas atoms. Further, the concentration of adsorbed oxygen atoms in the useful range of pressures is probably so large as to be almost independent of pressure. Hence it is concluded that the mechanism involving the solid state is the more nearly correct and that the source of a pressure dependence term is in the effect of pressure upon lattice defects.

If the connection between corrosion and electrical conduction of an ionic character is valid, then the value of ν in equation (VIII) should lie in the same range as μ. Waber (13), in a discussion of Gulbransen and Andrew's papers (14, 15), showed that the oxygen dependence of K_p for titanium and zirconium depends on approximately the 1/3 power of the pressure.

The pressure dependence of the conductivity of tantalum pentoxide has been examined by Hartman (16) who varied the oxygen pressure and detected a small increase in the conductivity, when vacuum-prepared samples were annealed in oxygen. Inasmuch as the tantalum is in its highest valence state, an increase due to oxygen would not be expected, although a decrease might be possible. The observed increase, however, may be due to the effect on impurities contained in the oxide. It was further shown by Hartman that annealing in hydrogen produced a significant increase in conductivity. For these reasons, it has been assumed that μ is zero for the conductivity relation. In the present case of tantalum the further assumption, based on the discussion above, has been made that ν is zero.

It is difficult to see how either of the mechanisms proposed to account for the logarithmic laws could show a strong dependence on the external pressure of the oxygen. In the absence of direct evidence, it

has been assumed that the rate constant K_1 is independent of pressure.

The low oxygen-dependence of rate constants K_p and K_1 in the two forms of the growth law makes it possible to neglect local exhaustion of oxygen in the immediate vicinity of solid-gas interface. The form of expression (VIII) permits evaluation of the energy of activation for the rate-controlling step, without the determination of ν. When the logarithm of the specific rate constant is plotted against the reciprocal of the absolute temperature a straight line results, if the reaction proceeds according to a rate law involving a single constant. The slope of this line is directly proportional to the energy of activation

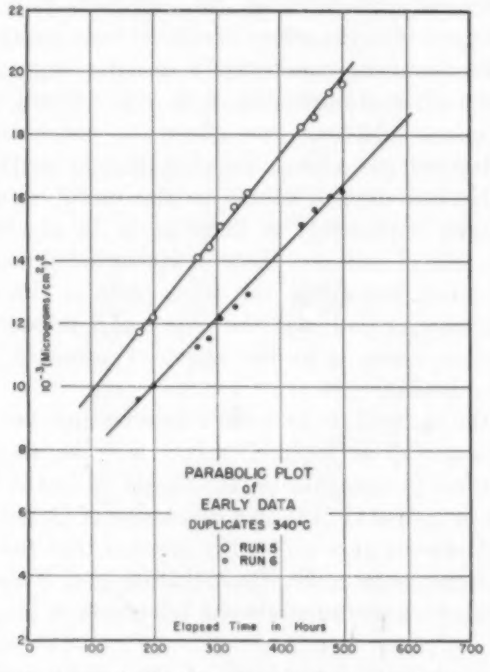

FIG. 4. A parabolic plot of early data, duplicate runs at 340°C.

for that process. The specific rate constant B may be replaced by K_p or K_1 in calculating the logarithmic form for the ordinate since the factor P^r cancels out when the slope is computed, as long as P is the same for each temperature used. Throughout the present investigation the specimens were exposed to air and hence the value of P is constant. Variations in the atmospheric pressure may be neglected also.

Because the rate of supply of tantalum ions is high near the metal-oxide interface it is likely that a layer of tantalum dioxide separates the metal from the pentoxide, and the stratified oxide layers may affect the rate and mechanism of oxidation. TaO is an "unsaturated" compound and cationic diffusion should be large in comparison with that through the pentoxide. Experience shows the reaction to be under diffusion control and it is logical to assume that oxidation would be controlled by the Ta_2O_5 layer. Valensi (17) has shown that the overall rate constant for cases involving stratified oxide layers does not differ markedly from the rate constant for oxidation of the outer layer and as would be expected the overall value converges to the rate constant appropriate to the oxide which is controlling. So it is concluded that the presence of dioxide does not affect the rate in the temperature range of this research. A specimen exposed at 350°C which exhibited the parabolic behavior was analyzed by x-rays. Only Ta_2O_5 and Ta were detected. So TaO was not present in a large amount near the surface. Hence the change from

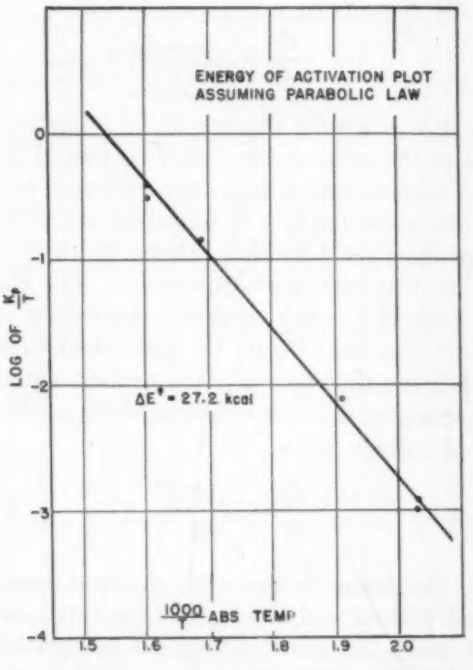

FIG. 5. Energy of activation plot assuming parabolic law

logarithmic to parabolic growth behavior cannot be attributed to change in composition of the oxide layers from mainly pentoxide to mainly dioxide as the temperature was increased[5].

KINETIC ANALYSIS OF PRESENT DATA

Gulbransen and Andrew (3) obtained an activation energy of 27.4 kcal/mole for the parabolic growth law in the temperature range 250° to 400°C. This agrees with that of the present investigation. Tantalum oxidation data suggest diffusion type control and a parabolic law, as seen from Fig. 4. The initial oxidation for all six samples seemed to agree well with the parabolic law. The logarithm of K_p/T against the reciprocal of temperature is plotted in

[5] Chemical evidence indicates that +2 state of tantalum is unstable and that TaO (or Ta_2O_2) is pyrophoric.

Fig. 5. This gave an activation energy of 27.2 kcal/mole as compared to 22.9 obtained from Balke's data (1).

Balke's data were based on the initial rates (i.e., the chord was drawn between zero and the weight after 24 hours). Although this fact alone may not explain the low value, a proper rate expression would tend to decrease the slope of chord line and thus reduce the corrosion rate.

Extended oxidation tests showed that the initial parabolic law was not satisfactory for expressing either the weight change or the change in thickness with time, as demonstrated by Fig. 6 and 7. This was particularly true at the lower temperatures. However, Fig. 1 and 2 indicated that good agreement

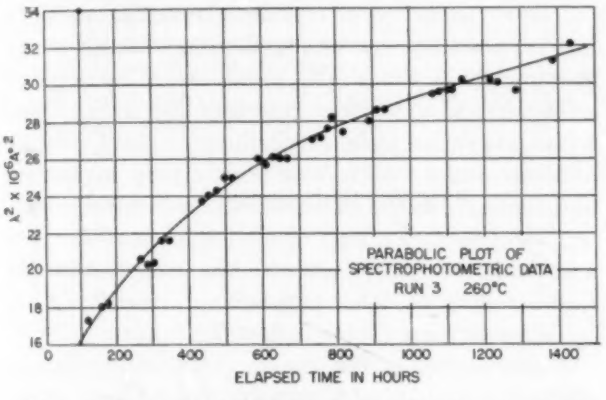

Fig. 6. Plot of weight gain data indicating the inadequacy of the parabolic law over an extended period.

was obtained over the temperature range with the logarithmic form of the rate equation. Arrhenius plots have been made of the reaction rate constants K_1 in equation (I) for both types of data. The slopes of the lines such as in Fig. 8 permitted evaluation of the "energies of activation" for the unknown rate-controlling step. They are:

Method	"Energy of activation"
Microgravimetric	12.57 kcal/mole
Spectrophotometric	12.0 kcal/mole

The spectrophotometric value is less accurate because of the partial overlapping of several orders of colors. The data obtained for rapid oxidation such as at 350°C show considerable spread (about 30%) and the $\Delta E^{\ddagger}$ is not more accurate than 12 kcal/mole. Nevertheless, the consistency between the two different methods is satisfactory.

The curves in Fig. 2 showed departures from the straight line, particularly at the longer times, suggesting a parabolic law fit. Deviation at early times is due to the error introduced by plotting the data against the logarithm of the elapsed time instead of adding the constant term onto the elapsed time before computing the logarithm [cf. equation (III)]. Fig. 9 shows that the data are in better agreement with a parabolic law.

In summary, the oxidation of tantalum in the temperature range below 320°C is unambiguously of the logarithmic type whereas that which occurs at

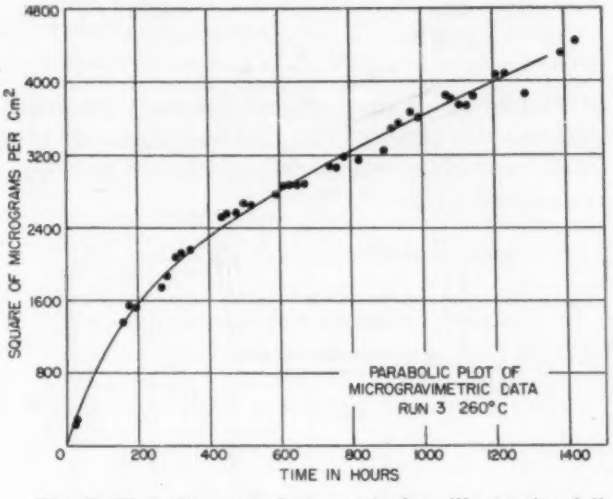

Fig. 7. Plot of spectrophotometric data illustrating failure of parabolic law over extended oxidation period.

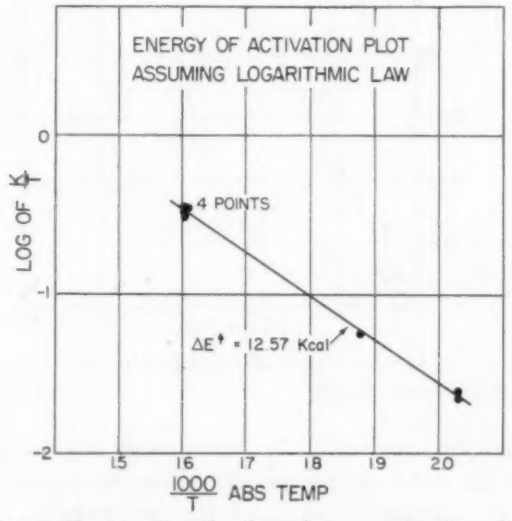

Fig. 8. Energy of activation plot assuming logarithmic law.

350°C is probably neither logarithmic nor parabolic but in that transition zone where both laws hold equally well and neither is exclusively correct. Such a transition between rate type has been noted elsewhere for aluminum (18) and magnesium (19).

Phase Shift

The equivalent phase shift δ can be calculated by Winterbottom's method (20). The value so obtained

agrees in magnitude with that obtained from the comparison plot, Fig. 3. These data are presented below:

Wavelength of light	Equivalent oxide thickness
4130 Å	62.5 Å
4430	82.5
4760	102.5
5100	122.5
5470	144.5
5820	162.5

In employing Winterbottom's method, the oxide thickness was obtained from the weight gain divided by the ratio of the true to the apparent surface areas, i.e., divided by ten.

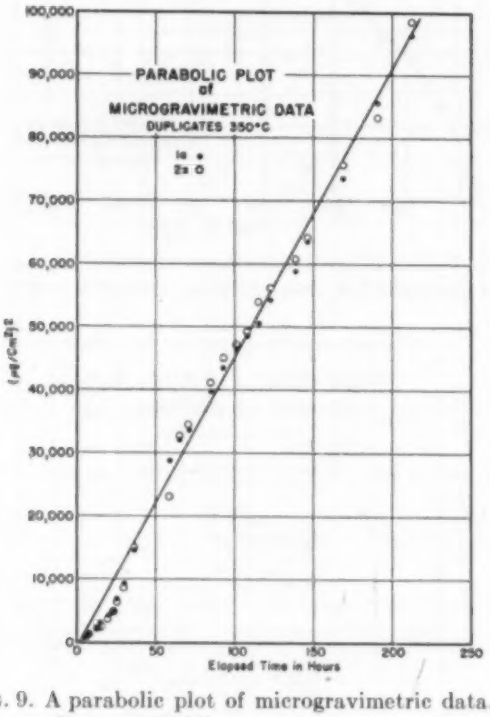

FIG. 9. A parabolic plot of microgravimetric data. Duplicate specimens at 350°C.

This variation of δ with wavelength is reasonable since the phase shift is usually some simple and relatively constant fraction of the wavelength. This variation may account for the slight curvature of the lines in Fig. 3.

REPRODUCIBILITY

The reproducibility of the results is surprisingly high for this type of heterogeneous reaction. Agreement of results within an order of magnitude is frequently considered good enough for practical use.

Typical of the reproducibility and precision is the total weight change for specimens 1A and 2A which agrees to better than 5 $\mu g/cm^2$ or 1 per cent after 212 hours. The average parabolic rate constant for quadruplicate samples in two separate runs at 350°C is 211.5 ± 4.3 $(\mu g/cm^2)^2/hr$. The probable error, rather than the standard deviation σ, leads to a coefficient of variance of better than 3 per cent. The ratio of surface areas was determined from three slopes of comparison curves (Fig. 3). The average value was 9.92 with a probable error of 0.079 or a coefficient of variance based on the probable error of eight tenths of a per cent.

Good agreement was also obtained between the energies of activation of the logarithmic growth. The $\Delta E^{\ddagger}$ values from spectrophotometric data gave 12 kcal and that from the microgravimetric data gave 12.57 kcal.

SUMMARY

The air oxidation of tantalum from 220° to 350°C has been studied by spectrophotometric and microgravimetric methods. The resistance of tantalum to oxidation and to thermal cycling of the oxide-covered metal was found to be excellent up to 320°C. Highly adherent scales were formed despite frequent heating and cooling. On the basis of data not included here, tantalum follows a logarithmic rate equation up to approximately 320°C. Above this temperature the rate law may be either parabolic or logarithmic but an unambiguous choice cannot be made.

A comparison of the results obtained by the two methods reveals good agreement. An estimate of the ratio of the true to the apparent surface area can be made from these data. The value of the ratio is 9.92 ± 0.07.

The energy of activation for the initial parabolic rates of weight change was found to be 27.2 kcal/mole, in good agreement with a previous value (14). The logarithmic growth laws gave straight lines on an Arrhenius plot. The "energy of activation" from the microbalance data was 12.57 kcal/mole, and that from the spectrophotometer was 12 kcal/mole.

The reproducibility was good for heterogeneous reaction. Triplicate determinations of surface area ratio were obtained with a "probable error" of 0.8 per cent and quadruplicate runs of the parabolic reaction rate constant gave a "probable error" of 3 per cent.

ACKNOWLEDGMENTS

The authors wish to express their gratitude and indebtedness to Dr. Eugene Staritzky of our Analytical Chemistry Group for his determination of refractive indexes and optical dispersion of tantalum pentoxide, to Dr. Joseph Singer of our Physical Metallurgy Group for his x-ray identification of the several films, and to Miss Santon Fotheringham and Mrs. B. P. Wellborn, also of the Physical Metallurgy Group, for their great assistance in preparing this

report. The helpful discussions of Drs. E. R. Jette and G. K. Rollefson, together with their suggestions for revising the manuscript, are gratefully acknowledged.

Note added in proof: New and improved x-ray evidence suggests that a phase other than Ta and Ta_2O_5 is present in oxidation products formed at 300°C and below.

Any discussion of this paper will appear in a Discussion Section, to be published in the December 1952 issue of the JOURNAL.

REFERENCES

1. C. BALKE, "Corrosion Handbook," (H. H. UHLIG, Editor), p. 721, J. Wiley & Sons, Inc., New York (1948).
2. D. J. MCADAMS AND G. W. GEIL, *J. Research Nat. Bur. Standards*, **23**, 65 (1935).
3. E. A. GULBRANSEN AND K. F. ANDREW, *J. (and Trans.) Electrochem. Soc.*, **96**, 364 (1949).
4. L. C. BANNISTER AND U. R. EVANS, *Proc. Roy. Soc. (London)*, **A125**, 370 (1929).
5. F. H. CONSTABLE, *Proc. Roy. Soc. (London)*, **A115**, 570 (1927).
6. F. H. CONSTABLE, *Ibid.*, **117**, 376 (1927-28).
7. L. TRONSTAD, *Z. physik. Chem.*, **A142** 241 (1929).
8. A. B. WINTERBOTTOM, *Trans. Electrochem. Soc.*, **76**, 327 (1939).
9. R. F. MEHL AND B. LUSTMAN, *Trans. Am. Inst. Mining Met. Engrs.*, **43**, 246 (1941).
10. U. R. EVANS, "Metallic Corrosion Passivity and Protection" p. 92 ff., Longmans Green, New York (1946).
11. F. J. WILKINS, *J. Chem. Soc.*, **1930**, 304.
12. C. WAGNER, "Pittsburgh International Conference on Surface Reactions," p. 80, Corrosion Publishing Co., Pittsburgh (1948).
13. J. T. WABER, Discussion of Ref. 14 and 15 by GULBRANSEN AND ANDREW.
14. E. A. GULBRANSEN AND K. F. ANDREW, *Am. Inst. Mining Met. Engrs., Tech. Pub. 2659* (1949).
15. E. A. GULBRANSEN AND K. F. ANDREW, *Am. Inst. Mining Met. Engrs., Tech. Pub. 2684* (1949).
16. W. Z. HARTMAN, *Z. Physik*, **102**, 709 (1936).
17. G. VALENSI, "Pittsburgh International Conference on Surface Reactions," p. 156, Corrosion Publishing Co., Pittsburgh (1948).
18. E. A. GULBRANSEN AND A. WYSONG, *J. Phys. & Colloid Chem.*, **51**, 1089 (1947).
19. E. A. GULBRANSEN, *Trans. Electrochem. Soc.*, **87**, 589 (1945).
20. A. B. WINTERBOTTOM, Appendix in Evans' book, Ref. 10, p. 814.

50 YEARS OF PHOSPHORUS IN CANADA

1897

Our phosphorus plant at Buckingham, Quebec

1951

showing 54 years of expansion in phosphorus production

1953

Electric Reduction is still expanding! In 1953 two 15,000 kw furnaces, the first additional units of our new plant at Varennes, Que., on the St. Lawrence, will be in production.

ELECTRIC REDUCTION SALES COMPANY LIMITED

TORONTO

137 WELLINGTON STREET WEST — PLANT AT BUCKINGHAM, QUEBEC